DOI:10.22337/2587-9618-2020-16-1-48-72

FINITE ELEMENTS OF THE PLANE PROBLEM OF THE THEORY OF ELASTICITY WITH DRILLING DEGREES OF FREEDOM

Viktor S. Karpilovskyi
ScadGroup Ltd., Kyiv, UKRAINE

Abstract: Twelve new finite elements with drilling degrees of freedom have been developed: triangular and quadrangular elements based on a modified hypothesis about the value of approximating functions on the sides of the element, which made it possible to avoid dimensional instability when all rotation angles are zero; incompatible and compatible triangular and quadrangular elements which can have additional nodes on the sides. Approximating functions satisfy the following condition: the value of the rotational degree of freedom of a node is nonzero and equal to one only for one of them. Numerical examples illustrate estimated minimum orders of convergence for displacements and stresses. All created elements retain the existing symmetry of the design models.

Keywords: finite elements, drilling degrees, plane problem, triangular element, rectangular element, quadrangular element

КОНЕЧНЫЕ ЭЛЕМЕНТЫ ПЛОСКОЙ ЗАДАЧИ ТЕОРИИ УПРУГОСТИ С ВРАЩАТЕЛЬНЫМИ СТЕПЕНЯМИ СВОБОДЫ

В.С. Карпиловский
ООО ScadGroup, г. Киев, УКРАИНА

Аннотация: Построено двенадцать новых конечных элементов с вращательными степенями свободы: треугольные и четырехугольные элементы на основе модифицированной гипотезы о значении аппроксимирующих функций на сторонах элемента, позволившей исключить геометрическую изменяемость при равенстве нулю всех углов поворота; несовместные и совместные треугольные и четырехугольные элементы, которые могут иметь дополнительные узлы на сторонах. При этом аппроксимирующие функции удовлетворяют условию: значение вращательной степени свободы узла только для одной из них отлично от нуля и равно единице. Приведены оценки минимальных порядков сходимости по перемещениям и напряжениям, иллюстрированные численными примерами. Все построенные элементы сохраняют существующую симметрию расчетных схем.

Ключевые слова: конечные элементы, вращательные степени свободы, плоская задача, треугольный элемент, прямоугольный элемент, четырехугольный элемент

1. INTRODUCTION

Let us consider the Lagrange functional of the plane problem of the theory of elasticity:

$$\Pi(\boldsymbol{u}) = \frac{1}{2}\int_{\Omega}(A\boldsymbol{u})^{T} DA\boldsymbol{u}d\Omega - \int_{\Omega}\boldsymbol{f}^{T}\boldsymbol{u}d\Omega \qquad (1)$$

where: Ω – plate of thickness h: solid body with a midplane ***XOY***;

$$\boldsymbol{u}(\boldsymbol{x}) = \begin{Bmatrix} \mathrm{u}(\boldsymbol{x}) \\ \mathrm{v}(\boldsymbol{x}) \end{Bmatrix}$$

– displacements of the point,

$$\boldsymbol{x}=\begin{Bmatrix}x\\y\end{Bmatrix},\quad \boldsymbol{f}(\boldsymbol{x})=\begin{Bmatrix}f_x(\boldsymbol{x})\\f_y(\boldsymbol{x})\end{Bmatrix}$$

– area load.

The geometry operator $\boldsymbol{A}$ and the elasticity matrix $\boldsymbol{D}$ (for an isotropic material) are:

$$\boldsymbol{A}^T=\begin{bmatrix}\frac{\partial}{\partial x} & 0 & \frac{\partial}{\partial y}\\ 0 & \frac{\partial}{\partial y} & \frac{\partial}{\partial x}\end{bmatrix},\quad \boldsymbol{D}=\frac{E}{1-\nu^2}\begin{bmatrix}1 & \nu & 0\\ \nu & 1 & 0\\ 0 & 0 & \frac{1-\nu}{2}\end{bmatrix}, \quad (2)$$

E – Young's modulus, ν – Poisson's ratio.

Classic finite elements have two degrees of freedom in each node: nodal displacements u_i, v_i, i=1,2,…,N, where N is the number of element nodes. There are also more complex elements with three degrees of freedom in a node, when the following values can be taken into account in addition to the displacement values:

- averaged rotation angle:

$$\omega_i=\omega_z(\boldsymbol{x}_i),\quad \omega_z=\frac{1}{2}\left(\frac{\partial v}{\partial x}-\frac{\partial u}{\partial y}\right) \quad (3)$$

According to [1] the value ω_z characterizes the rotation of an infinitesimal volume surrounding a point. This value is invariant with respect to orthogonal transformations of coordinate systems.

- the paper [2] proposes and the papers [3-5 et al.] develop the approach when the degrees of freedom θ_j with the following hypotheses are introduced at the nodes:

a) tangential displacement u_τ varies linearly on the side ij;

b) normal displacement u_n varies according to the law:

$$\mathrm{u}_n=(1-\xi)\mathrm{u}_{ni}+\xi u_{nj}+\frac{a_{ij}}{2}(\theta_j-\theta_i)\xi(1-\xi), \quad (4)$$
$$\boldsymbol{x}=\boldsymbol{x}_i+\xi(\boldsymbol{x}_j-\boldsymbol{x}_i),\quad \boldsymbol{\tau}_{ij}=(\boldsymbol{x}_j-\boldsymbol{x}_i)/a_{ij}$$
$$a_{ij}=|\boldsymbol{x}_j-\boldsymbol{x}_i|$$

– side length;

- in order to avoid dimensional instability which can occur when all degrees of freedom are equal θ_j according to the hypothesis (4), we will assume that the normal displacement u_n varies according to the law proposed in [6]:

$$u_n=(1-\xi)\mathrm{u}_{ni}+\xi u_{nj}+\frac{a_{ij}}{2}\xi(1-\xi)\left(\theta_j-\theta_i+\varepsilon(\theta_j+\theta_i)(1-2\xi)\right), \quad (5)$$

ε=const.

Degrees of freedom θ_j, created according to the hypothesis (5) will be called ***quasi-rotational***. And for the function $\boldsymbol{\varphi}_i(\boldsymbol{x})$, corresponding to the degree of freedom $\boldsymbol{\theta}_i$:

$$\omega_z(\boldsymbol{\varphi}_i(\boldsymbol{x}))\Big|_{\boldsymbol{x}_j}=\begin{cases}0.5(1-\varepsilon), & i=j,\\ -0.25(1+\varepsilon), & i\neq j, \text{ side}\\ 0, & i\neq j, \text{ diagonal}\end{cases} \quad (6)$$

If we substitute $\varepsilon=-1$ into (6), we obtain:

$$u_n=(1-\xi)\mathrm{u}_{ni}+(1-\xi)\mathrm{u}_{nj}+a_{ij}\xi(1-\xi)(\theta_j\xi-\theta_i(1-\xi)) \quad (7)$$

and $\omega_z(\boldsymbol{\varphi}_i(\boldsymbol{x}))|_{\boldsymbol{x}_j}=\delta_i^j$, i,j=1,2,…,N.

The direction of the normal vector to the side $\boldsymbol{n}_{ij}$ for (4) and (5) is selected in such a way so that the system $\boldsymbol{n}_{ij}$, $\boldsymbol{\tau}_{ij}$ and $\boldsymbol{OZ}$ is right-hand. The *compatibility* of the respective system of approximating functions is provided in both cases.

However, (4) has the following disadvantages:

a) since the degrees of freedom θ_j in (4) are included only as a difference between the values on the sides, it is necessary to create additional constraints in order to avoid degeneracy of the system or to introduce fictitious rigidities;

b) the calculated values θ_j can be quite far from the actual rotation angles.

Additional constraints are not required for (5). As shown by numerical experiments we obtain

good accuracy of the results for small values of ε, which almost coincides with that of the results for displacements and stresses with the elements according to the hypothesis (4). The values of the "rotation angles" θ_j are more realistic.

For hypotheses (4) and (5):

a) moment loads are ***incorrect***;

b) when creating elements with intermediate nodes on the sides, it is almost impossible to agree the physical meaning of θ_j at the vertices and on the sides. Therefore, θ_j are either not determined on the sides as in [7], or are determined artificially as in [8].

The degrees of freedom θ_j for (4) and (5) no longer have an exact physical meaning. They can hardly be interpreted as ***"rotation angles"***. However, the corresponding approximating functions do not contradict the ideology of the FEM as a projection-grid method and show good results in shell analysis.

A large number of elements with rotational degrees of freedom based on formulations other than the Lagrange functional were created: hybrid elements based on a mixed functional [9], elements based on the Trefftz method [10], on the expansion by displacement modes [11] etc. [12,13,14 at al.]. The list of publications on this subject is obviously not complete. The elements considered in this paper are based on the Lagrange functional.

As confirmed by numerical experiments, the load can be given as moments: both nodal and distributed over an element (for example, along the side), for elements which have degrees of freedom ω_z and ensure convergence of the method. The reduced nodal moments are calculated according to a standard formula:

$$M_i = \int_{\Omega} M(x,y)\omega_z(\boldsymbol{\varphi}_i)d\Omega \qquad (8)$$

When there are three degrees of freedom in a node, finite elements have 3N unknowns, which are arranged in the following order during the generation of a stiffness matrix of the element:

$$\{u_1, v_1, \omega_1 ..., u_N, v_N, \omega_N\} \text{ and, accordingly,}$$
$$\{u_1, v_1, \theta_1 ..., u_N, v_N, \theta_N\}, \qquad (9)$$

which have a corresponding system of approximating functions:

$$\left\{ \boldsymbol{\varphi}_{ij}(x,y),\ \boldsymbol{\varphi}_{ij} = \begin{Bmatrix} \varphi_{ij,u} \\ \varphi_{ij,v} \end{Bmatrix},\ i = 1 \div N,\ j = 1,2,3 \right\} \qquad (10)$$

For example, the displacement field for the degrees of freedom θ_j is represented as:

$$\boldsymbol{u}(x,y) = \sum_{i=1}^{N} (u_i \boldsymbol{\varphi}_{i1} + v_i \boldsymbol{\varphi}_{i2} + \theta_i \boldsymbol{\varphi}_{i3}) = \sum_{i=1}^{N} \begin{Bmatrix} u_i \varphi_{i1,u} + v_i \varphi_{i2,u} + \theta_i \varphi_{i3,u} \\ u_i \varphi_{i1,v} + v_i \varphi_{i2,v} + \theta_i \varphi_{i3,v} \end{Bmatrix}, \qquad (11)$$

Functions satisfying (5) will be represented as follows:

$$\boldsymbol{\varphi}_{i3}(\boldsymbol{x}) = \boldsymbol{\chi}_i(\boldsymbol{x}) + \varepsilon \boldsymbol{\zeta}_i(\boldsymbol{x}), \quad i=1,2,\ldots,N, \qquad (12)$$

where $-\ \boldsymbol{\chi}_i$ functions obtained from hypothesis (4), $\boldsymbol{\zeta}_i$ – correction functions.

Let us introduce the notation L_{ij} for operators of degrees of freedom:

$$L_{i1}(\boldsymbol{\varphi}(\boldsymbol{x})) = \varphi_u(\boldsymbol{x}_i),\quad L_{i2}(\boldsymbol{\varphi}(\boldsymbol{x})) = \varphi_v(\boldsymbol{x}_i),$$
$$L_{i3}(\boldsymbol{\varphi}(\boldsymbol{x})) = \omega_z(\boldsymbol{\varphi}(\boldsymbol{x}))|_{\boldsymbol{x}_i},\quad i = 1,2,\ldots,N. \qquad (13)$$

For i=1,2 – these are nodal displacements in the respective directions.

The following condition has to be satisfied:

$$L_{ij}(\boldsymbol{\varphi}_{km}(\boldsymbol{x})) = \delta_{ij}^{km},\ i=1,2,\ldots,N, \qquad (14)$$

j=1,2 for (4) and (5) and j=1,2,3 for ω_z.

Convergence criteria

Criteria for proving the convergence of both compatible and incompatible finite elements for problems with elliptic differential equilibrium equations of arbitrary order were proposed in

[15–17] and were used in [15] to create new elements.

Let us formulate them for the plane problem of the theory of elasticity. Equalities of the completeness criterion of the minimum order for the degrees of freedom u_i, v_i, ω_i:

$$\begin{aligned}
&\sum_{i=1}^{N}\boldsymbol{\varphi}_{i1}(\boldsymbol{x})\equiv\begin{Bmatrix}1\\0\end{Bmatrix},\qquad \sum_{i=1}^{N}x_i\boldsymbol{\varphi}_{i1}(\boldsymbol{x})\equiv\begin{Bmatrix}x\\0\end{Bmatrix},\\
&\sum_{i=1}^{N}\left(y_i\boldsymbol{\varphi}_{i1}(\boldsymbol{x})+\boldsymbol{\varphi}_{i3}(\boldsymbol{x})\right)\equiv\begin{Bmatrix}y\\0\end{Bmatrix},\\
&\sum_{i=1}^{N}\boldsymbol{\varphi}_{i2}(\boldsymbol{x})\equiv\begin{Bmatrix}0\\1\end{Bmatrix},\qquad \sum_{i=1}^{N}y_i\boldsymbol{\varphi}_{i2}(\boldsymbol{x})\equiv\begin{Bmatrix}0\\y\end{Bmatrix},\\
&\sum_{i=1}^{N}\left(x_i\boldsymbol{\varphi}_{i2}(\boldsymbol{x})-\boldsymbol{\varphi}_{i3}(\boldsymbol{x})\right)\equiv\begin{Bmatrix}0\\x\end{Bmatrix}
\end{aligned}\qquad (15)$$

Conditions (15) must be satisfied for the approximations according to (4) and (5), if we assume that $\boldsymbol{\varphi}_{i3}$= 0. Adding independent approximations can only increase the order of the completeness criterion.

When (15) is satisfied, it guarantees the displacement of a finite element as a rigid body, and for compatible approximations according to [15,16], the method will converge in displacements with the 2-nd order, and in stresses with the 1-st order.

An *incompatibility criterion* is introduced for incompatible approximating functions. For the considered problem it lies in finding such a compatible system of functions

$$\left\{\ \boldsymbol{\psi}_{ij}(x,y),\ \ i=1,2,...N,\ \ j=1,2,3\ \right\}\ , \qquad (16)$$

that must guarantee the displacement of the finite element as a rigid body (or the fulfillment of all equalities (14), which are more strict conditions) and satisfy the equations

$$\int_{\Omega}\begin{bmatrix}\frac{\partial}{\partial x} & \frac{\partial}{\partial y} & 0 & 0\\ 0 & 0 & \frac{\partial}{\partial x} & \frac{\partial}{\partial y}\end{bmatrix}^{T}(\boldsymbol{\varphi}_{ij}-\boldsymbol{\psi}_{ij})d\Omega=\begin{Bmatrix}0\\0\\0\\0\end{Bmatrix},\qquad (17)$$

i=1,2,…,N, j=1,2,3.

When performing (15) and (17) for incompatible approximations, according to [15,16], the method will converge in displacements with the 2-nd order, and in stresses with the 1-st order. When analyzing incompatible approximations for elements with rotational degrees of freedom, approximations of classic elements with two degrees of freedom of a node can be used as a compatible system of functions (16). The incompatibility criterion enables to analyze the approximations for one finite element unlike the piecewise testing [18,19,20], which requires the analysis of all possible stars of elements.

Functions for some nodes corresponding to the rotational degrees of freedom ω_z will be determined as follows for some elements:

$$\boldsymbol{\varphi}_{i3}(\boldsymbol{x})=\boldsymbol{\mu}_i(\boldsymbol{x})+\boldsymbol{\lambda}_i(\boldsymbol{x}),\qquad (18)$$

where $\boldsymbol{\mu}_i(\boldsymbol{x})$ and $\boldsymbol{\lambda}_i(\boldsymbol{x})$ are *compatible* and *incompatible* approximations, respectively.

It follows from the incompatibility criterion (17) that $\boldsymbol{\lambda}_i(\boldsymbol{x})$ must satisfy the equations:

$$\int_{\Omega}\begin{bmatrix}\frac{\partial}{\partial x} & \frac{\partial}{\partial y} & 0 & 0\\ 0 & 0 & \frac{\partial}{\partial x} & \frac{\partial}{\partial y}\end{bmatrix}^{T}\boldsymbol{\lambda}_{ij}(\boldsymbol{x})d\Omega==\begin{Bmatrix}0\\0\\0\\0\end{Bmatrix}\qquad (19)$$

The aim of the work is to build 12 new finite elements with rotational degrees of freedom using the above convergence criteria, ensuring the convergence of the finite element method.

2. FINITE ELEMENTS

2.1. Finite Elements with Quasi-rotational Degrees of Freedom

a) Three-node Element

Let us consider a triangle in the local coordinate system shown in Figure 1a. After changing the coordinates (20), it is transformed into a right triangle with unit legs shown in Figure 1b.

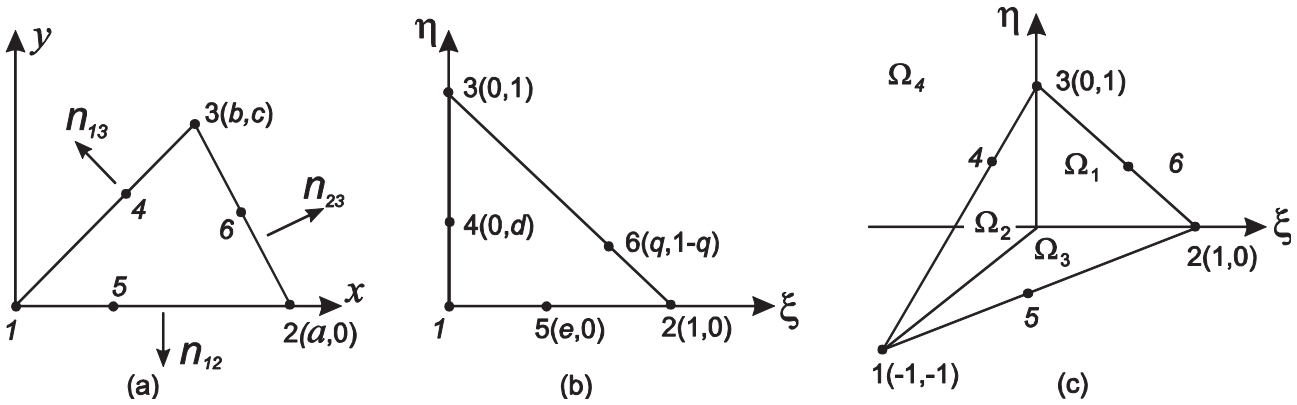

Figure 1. Triangular element.

$$\xi = \frac{1}{a}\left(x - \frac{b}{c} y \right), \quad \eta = \frac{1}{c} y \tag{20}$$

We will determine the degrees of freedom only at the vertices of the triangle.
Normal's to the element sides:

$$\boldsymbol{n}_{12} = \begin{Bmatrix} 0 \\ -1 \end{Bmatrix}, \quad \boldsymbol{n}_{13} = \frac{1}{a_{13}} \begin{Bmatrix} -c \\ b \end{Bmatrix}, \quad \boldsymbol{n}_{23} = \frac{1}{a_{23}} \begin{Bmatrix} c \\ a-b \end{Bmatrix}$$

The following approximation of displacements in the form (12) satisfies the conditions (5):

$$\boldsymbol{\varphi}_{i1}(\boldsymbol{x}) = \{\psi_i, 0\}^T, \quad \boldsymbol{\varphi}_{i2}(\boldsymbol{x}) = \{0, \psi_i\}^T \tag{21}$$

$$\psi_1 = 1 - \xi - \eta, \quad \psi_2 = \xi, \quad \psi_3 = \eta, \; i=1,2,3$$

$$\boldsymbol{\chi}_1 = \frac{1-\xi-\eta}{2} \begin{Bmatrix} -c\eta \\ a\xi + b\eta \end{Bmatrix}, \; \boldsymbol{\chi}_2 = \frac{\xi}{2} \begin{Bmatrix} -c\eta \\ -a(1-\xi) + b\eta \end{Bmatrix}$$

$$\boldsymbol{\chi}_3 = \frac{\eta}{2} \begin{Bmatrix} c(1-\eta) \\ a\xi - b(1-\eta) \end{Bmatrix} \tag{22}$$

$$\boldsymbol{\zeta}_1 = \frac{1-\xi-\eta}{2} \begin{Bmatrix} -c\eta(\xi + 2\eta - 1)] \\ -a\xi(1-2\xi-\eta) - b\eta(1-\xi-2\eta) \end{Bmatrix},$$

$$\boldsymbol{\zeta}_2 = \frac{\xi}{2} \begin{Bmatrix} c\eta(\xi-\eta] \\ b\eta(\eta-\xi) - a(H-\xi) \end{Bmatrix},$$

$$\boldsymbol{\zeta}_3 = \frac{\eta}{2} \begin{Bmatrix} c(H-\eta) \\ a\xi(\xi-\eta) - b(H-\eta) \end{Bmatrix}, \tag{23}$$

$$H(\xi,\eta) = 1 - 2\xi - 2\eta + 2\xi^2 + 2\xi\eta + 2\eta^2$$

Functions (22) – approximations [2].

b) Four-node Isoparametric Element

Let us consider a convex quadrangular finite element in the local coordinate system shown in Figure 2a. After an isoparametric transformation of the coordinate system (24), it is transformed into a unit square shown in Figure 2b.

$$\begin{aligned} x &= a\xi(1-\eta) + b(1-\xi)\eta + d\xi\eta, \\ y &= c(1-\xi)\eta + e\xi\eta \end{aligned} \tag{24}$$

Normals to the sides:

$$\boldsymbol{n}_{12} = \begin{Bmatrix} 0 \\ -1 \end{Bmatrix}, \qquad \boldsymbol{n}_{24} = \frac{1}{a_{24}} \begin{Bmatrix} e \\ a-d \end{Bmatrix},$$

$$\boldsymbol{n}_{34} = \frac{1}{a_{34}} \begin{Bmatrix} c-e \\ d-b \end{Bmatrix}, \; \boldsymbol{n}_{13} = \frac{1}{a_{13}} \begin{Bmatrix} -c \\ b \end{Bmatrix}$$

We will determine the degrees of freedom only at the vertices of the quadrangle.
The following approximation of displacements in the form (12) satisfies the conditions (5):

$$\boldsymbol{\varphi}_{i1}(\boldsymbol{x}) = \begin{Bmatrix} 0 \\ \psi_i \end{Bmatrix}, \; \boldsymbol{\varphi}_{i2}(\boldsymbol{x}) = \begin{Bmatrix} \psi_i \\ 0 \end{Bmatrix}, \; =1,2,3,4, \tag{25}$$

$$\begin{aligned} \psi_1 &= (1-\xi)(1-\eta), \quad & \psi_2 &= \xi(1-\eta), \\ \psi_3 &= (1-\xi)\eta, & \psi_4 &= \xi\eta \end{aligned}$$

$$\boldsymbol{\varphi}_{13} = \frac{(1-\eta)(1-\xi)}{2} \begin{Bmatrix} -c\eta \\ b\eta + a\xi \end{Bmatrix},$$

$$\boldsymbol{\varphi}_{23} = \frac{\xi(1-\eta)}{2} \begin{Bmatrix} -e\eta \\ -a(1-\xi) + (d-a)\eta \end{Bmatrix},$$

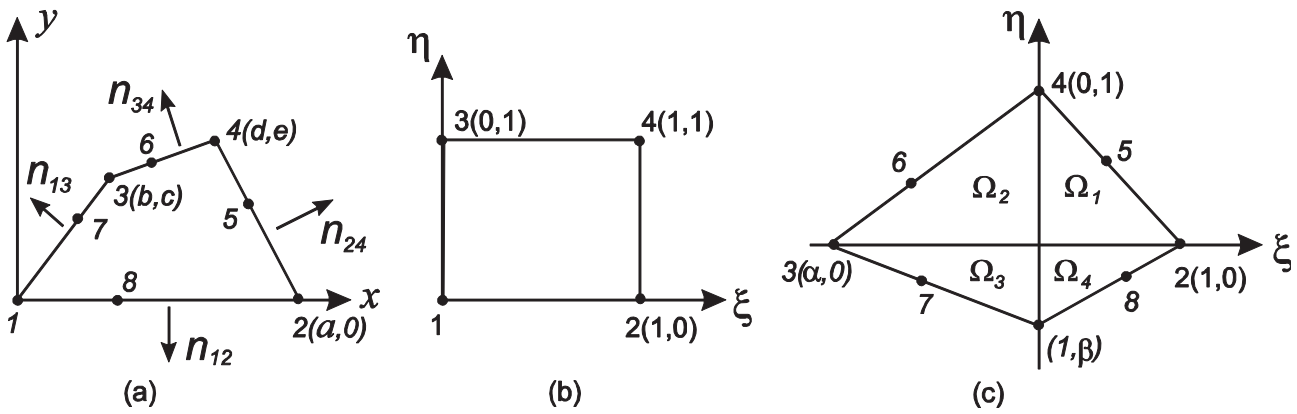

Figure 2. Quadrangular element.

$$\boldsymbol{\varphi}_{33}=\frac{(1-\xi)\eta}{2}\begin{Bmatrix}c(1-\eta)+(c-e)\xi\\(d-b)\xi-b(1-\eta)\end{Bmatrix},$$

$$\boldsymbol{\varphi}_{43}=\frac{\xi\eta}{2}\begin{Bmatrix}e(1-\eta)+(e-c)(1-\xi)\\(b-d)(1-\xi)+(a-d)(1-\eta)\end{Bmatrix} \qquad (26)$$

Functions (26) – approximations [4].

$$\boldsymbol{\zeta}_1(\boldsymbol{x})=\frac{(1-\xi)(1-\eta)}{2}\begin{Bmatrix}c\eta(1-2\eta)\\-b\eta(1-2\eta)-a\xi(1-2\xi)\end{Bmatrix},$$

$$\boldsymbol{\zeta}_2(\boldsymbol{x})=\frac{\xi(1-\eta)}{2}\begin{Bmatrix}e\eta(1-2\eta)\\a(\xi-1)(1-2\xi)-(d-a)\,\eta(1-2\eta)\end{Bmatrix},$$

$$\boldsymbol{\zeta}_3(\boldsymbol{x})=\frac{(1-\xi)\eta}{2}\begin{Bmatrix}c(1-\eta)(1-2\eta)-(c-e)\xi(1-2\xi)\\(b-d)\xi(1-2\xi)-b(1-\eta)(1-2\eta))\end{Bmatrix},$$

$$\boldsymbol{\zeta}_4(\boldsymbol{x})=\frac{\xi\eta}{2}\begin{Bmatrix}e(1-\eta)(1-2\eta)+\\\qquad(e-c)(1-\xi)(1-2\xi)\\(b-d)(1-\xi)(1-2\xi)+\\\qquad(a-d)(1-\eta)(1-2\eta)\end{Bmatrix} \qquad (27)$$

Two more functions are sometimes added which correspond to some internal degrees of freedom with their subsequent condensation:

$$\boldsymbol{\psi}_1=\{\xi(1-\xi)\eta(1-\eta),\ 0\}^T,$$
$$\boldsymbol{\psi}_2=\{0,\ \xi(1-\xi)\eta(1-\eta)\}^T$$

c) Four-node Element with a Piecewise Polynomial Approximation

Let us consider a quadrangular finite element in the local coordinate system shown in Figure 2a. It is transformed into a quadrangle shown in Figure 2c by replacing the coordinate system (28). A is the intersection point of the diagonals of the element.

$$\begin{cases}x=x_A+(a-x_A)\xi+(d-x_A)\eta\\y=y_{\mathbf{A}}(1-\xi)+(e-y_A)\eta\end{cases}, \qquad (28)$$

$$\begin{cases}\xi=p_{11}x+p_{12}y\\\eta=p_{21}x+p_{22}y+\beta\end{cases}$$

$$p_{11}=\frac{1}{a},\ p_{12}=-\frac{d}{ae},\ p_{21}=\frac{c}{\Delta},\ p_{22}=\frac{a-b}{\Delta},$$

$$\alpha=\frac{eb-dc}{\mathrm{ac}},\ \beta=-\frac{ac}{\Delta},\ \Delta=c(d-a)(a-b)e,$$

$$A=1/\alpha,\qquad B=1/\beta,$$

$$A_1=1/(1-\alpha),\ B_1=1/(1-\beta)$$

If the quadrangle is a rectangle, then $\alpha=\beta=-1$.

Let us consider functions (29) ψ_i, $i=1\div8$, which are second-degree polynomials in each of the subareas Ω_i, $i=1,2,3,4$ and are *continuous together with their first derivatives* on the diagonals of the element:

$$\psi_1=\frac{B_1}{2}\begin{cases}1-2\eta-\xi^2+\eta^2, & \boldsymbol{x}\in\Omega_1\\1-2\eta-A^2\xi^2+\eta^2, & \boldsymbol{x}\in\Omega_2\\1-2\eta-A^2\xi^2+B^2\eta^2, & \boldsymbol{x}\in\Omega_3\\1-2\eta-\xi^2+B^2\eta^2, & \boldsymbol{x}\in\Omega_4\end{cases},\quad \psi_2=\frac{A_1}{2}\begin{cases}-\alpha+2\xi-\alpha\xi^2+\alpha\eta^2, & \boldsymbol{x}\in\Omega_1\\-\alpha+2\xi-A\xi^2+\alpha\eta^2, & \boldsymbol{x}\in\Omega_2\\-\alpha+2\xi-A\xi^2+\alpha B^2\eta^2, & \boldsymbol{x}\in\Omega_3\\-\alpha+2\xi-\alpha\xi^2+\alpha B^2\eta^2, & \boldsymbol{x}\in\Omega_4\end{cases}$$

$$\psi_3=\frac{A_1}{2}\begin{cases}1-2\xi+\xi^2-\eta^2, & \boldsymbol{x}\in\Omega_1\\ 1-2\xi+A^2\xi^2-\eta^2, & \boldsymbol{x}\in\Omega_2\\ 1-2\xi+A^2\xi^2-B^2\eta^2, & \boldsymbol{x}\in\Omega_3\\ 1-2\xi+\xi^2-B^2\eta^2, & \boldsymbol{x}\in\Omega_4\end{cases},\ \psi_4=\frac{B_1}{2}\begin{cases}-\beta+2\eta+\beta\xi^2-\beta\eta^2, & \boldsymbol{x}\in\Omega_1\\ -\beta+2\eta+A^2\beta\xi^2-\beta\eta^2, & \boldsymbol{x}\in\Omega_2\\ -\beta+2\eta+A^2\beta\xi^2-B\eta^2, & \boldsymbol{x}\in\Omega_3\\ -\beta+2\eta+\beta\xi^2-B\eta^2, & \boldsymbol{x}\in\Omega_4\end{cases}$$

$$\psi_5=A_1B_1\begin{cases}2\alpha\beta-4\beta\xi-4\alpha\eta+2\beta(2-\alpha)\xi^2+4\xi\eta+2\alpha(2-\beta)\eta^2, & \boldsymbol{x}\in\Omega_1\\ 2\alpha\beta-4\beta\xi-4\alpha\eta+2A\beta\xi^2+4\xi\eta+2\alpha(2-\beta)\eta^2, & \boldsymbol{x}\in\Omega_2\\ 2\alpha\beta-4\beta\xi-4\alpha\eta+2A\beta\xi^2+4\xi\eta+2\alpha B\eta^2, & \boldsymbol{x}\in\Omega_3\\ 2\alpha\beta-4\beta\xi-4\alpha\eta+2\beta(2-\alpha)\xi^2+4\xi\eta+2\alpha B\eta^2, & \boldsymbol{x}\in\Omega_4\end{cases}$$

$$\psi_6=A_1B_1\begin{cases}-2\beta+4\beta\xi+4\eta-2\beta\xi^2-4\xi\eta-(4-2\beta)\eta^2, & \boldsymbol{x}\in\Omega_1\\ -2\beta+4\beta\xi+4\eta-A\beta(4-2A)\xi^2-4\xi\eta-(4-2\beta)\eta^2, & \boldsymbol{x}\in\Omega_2\\ -2\beta+4\beta\xi+4\eta-A\beta(4-2A)\xi^2-4\xi\eta-2B\eta^2, & \boldsymbol{x}\in\Omega_3\\ -2\beta+4\beta\xi+4\eta-2\beta\xi^2-4\xi\eta-4\xi\eta-2B\eta^2, & \boldsymbol{x}\in\Omega_4\end{cases}$$

$$\psi_7=A_1B_1\begin{cases}-2-4\xi-4\eta+2\xi^2+4\xi\eta+2\eta^2, & \boldsymbol{x}\in\Omega_1\\ -2-4\xi-4\eta-2A^2(1-2\alpha)\xi^2+4\xi\eta+2\eta^2, & \boldsymbol{x}\in\Omega_2\\ -2-4\xi-4\eta-2A^2(1-2\alpha)\xi^2+4\xi\eta-2B^2(1-2\beta)\eta^2, & \boldsymbol{x}\in\Omega_3\\ -2-4\xi-4\eta+2\xi^2+4\xi\eta-2B^2(1-2\beta)\eta^2, & \boldsymbol{x}\in\Omega_4\end{cases}$$

$$\psi_8=A_1B_1\begin{cases}-2\alpha+4\xi+4\alpha\eta-(4-2\alpha)\xi^2-4\xi\eta-2\alpha\eta^2, & \boldsymbol{x}\in\Omega_1\\ -2\alpha+4\xi+4\alpha\eta-2A\xi^2-4\xi\eta-2\alpha\eta^2, & \boldsymbol{x}\in\Omega_2\\ -2\alpha+4\xi+4\alpha\eta-2A\xi^2-4\xi\eta-\alpha B(4-2B)\eta^2, & \boldsymbol{x}\in\Omega_3\\ -2\alpha+4\xi+4\alpha\eta-(4-2\alpha)\xi^2-4\xi\eta-\alpha B(4-2B)\eta^2, & \boldsymbol{x}\in\Omega_4\end{cases} \tag{29}$$

Since $\boldsymbol{\psi}_i(\boldsymbol{x}_j)=\delta_i^j$, i,j=1,2,3,4, we can assign

$$\boldsymbol{\varphi}_{i1}(\boldsymbol{x})=\begin{Bmatrix}\psi_i\\0\end{Bmatrix},\quad \boldsymbol{\varphi}_{i2}(\boldsymbol{x})=\begin{Bmatrix}0\\\psi_i\end{Bmatrix},\quad i=1,2,3,4 \tag{30}$$

The functions ψ_i, i=5,6,7,8 at the vertices of the quadrangle are equal to zero. They are nonzero at the middle of the sides and equal to one only at the node with a number matching that of the function. The following expression is obtained in (12) for functions corresponding to quasi-rotational degrees of freedom and satisfying conditions (5):

$$\boldsymbol{\chi}_1=\frac{1}{8}\begin{Bmatrix}-c\psi_7\\ b\psi_7+a\psi_8\end{Bmatrix},\quad \boldsymbol{\chi}_2=\frac{1}{8}\begin{Bmatrix}-e\psi_5\\ -a\psi_8+(d-a)\psi_5\end{Bmatrix},$$

$$\boldsymbol{\chi}_3=\frac{1}{8}\begin{Bmatrix}c\psi_7+(c-e)\psi_6\\ (d-b)\psi_6-b\psi_7\end{Bmatrix},$$

$$\boldsymbol{\chi}_4=\frac{1}{8}\begin{Bmatrix}e\psi_5+(e-c)\psi_6\\ (b-d)\psi_6+(a-d)\psi_5\end{Bmatrix} \tag{31}$$

$$\boldsymbol{\zeta}_1=\frac{1}{8}\begin{Bmatrix}-c\psi_7(A\xi-B\eta)\\ b\psi_7(A\xi-B\eta)-a\psi_8(B\eta-\xi)\end{Bmatrix},$$

$$\boldsymbol{\zeta}_2=\frac{1}{8}\begin{Bmatrix}e\psi_5(\xi-\eta)\\ -a\psi_8(B\eta-\xi)-(d-a)\psi_5(\xi-\eta)\end{Bmatrix},$$

$$\boldsymbol{\zeta}_3=\frac{1}{8}\begin{Bmatrix}-c\psi_7(A\xi-B\eta)+(c-e)\psi_6(\eta-A\xi)\\ (d-b)\psi_6(\eta-A\xi)+b\psi_7(A\xi-B\eta)\end{Bmatrix},$$

$$\boldsymbol{\zeta}_4=\frac{1}{8}\begin{Bmatrix}e\psi_5(\xi-\eta)-(e-c)\psi_6(\eta-A\xi)\\ -(b-d)\psi_6(\eta-A\xi)+\\ \qquad(a-d)\psi_5(\xi-\eta)\end{Bmatrix} \tag{32}$$

2.2. Incompatible Finite Elements (ω_z)

d) Triangle with Nodes at Vertices

Let us consider a triangle shown in Fig. 1a, which is transformed into a triangle in Fig. 1b by replacing the coordinates (20). The system of approximating functions of an element will be sought as third-degree polynomials in the finite element area. We will determine the degrees of freedom only at the vertices of the triangle.

Consider auxiliary functions corresponding to the rotational degrees of freedom obtained from $\boldsymbol{\zeta}_i(\boldsymbol{x})$ in (27) and satisfying (14):

$$\boldsymbol{\lambda}_i(\boldsymbol{x}) = -4\boldsymbol{\zeta}_i(\boldsymbol{x}) + \boldsymbol{\zeta}(\boldsymbol{x}),\ i=1,2,3, \qquad (33)$$
$$\boldsymbol{\zeta}(\boldsymbol{x}) = \boldsymbol{\zeta}_1(\boldsymbol{x}) + \boldsymbol{\zeta}_2(\boldsymbol{x}) + \boldsymbol{\zeta}_3(\boldsymbol{x})$$

We adjust the functions (21) corresponding to the linear degrees of freedom of the classic element, so that the equalities (14) are satisfied:

$$\boldsymbol{\varphi}_{11}(\boldsymbol{x}) = \begin{Bmatrix} 1-\xi-\eta \\ 0 \end{Bmatrix} - \frac{a-b}{2ac}\boldsymbol{\zeta}(\boldsymbol{x}),$$
$$\boldsymbol{\varphi}_{12}(\boldsymbol{x}) = \begin{Bmatrix} 0 \\ 1-\xi-\eta \end{Bmatrix} + \frac{1}{2a}\boldsymbol{\zeta}(\boldsymbol{x}),$$
$$\boldsymbol{\varphi}_{21}(\boldsymbol{x}) = \begin{Bmatrix} \xi \\ 0 \end{Bmatrix} - \frac{b}{2ac}\boldsymbol{\zeta}(\boldsymbol{x}),\ \boldsymbol{\varphi}_{22}(\boldsymbol{x}) = \begin{Bmatrix} 0 \\ \xi \end{Bmatrix} - \frac{1}{2a}\boldsymbol{\zeta}(\boldsymbol{x}),$$
$$\boldsymbol{\varphi}_{31}(\boldsymbol{x}) = \begin{Bmatrix} \eta \\ 0 \end{Bmatrix} + \frac{1}{2c}\boldsymbol{\zeta}(\boldsymbol{x}),\quad \boldsymbol{\varphi}_{32}(\boldsymbol{x}) = \begin{Bmatrix} 0 \\ \eta \end{Bmatrix} \qquad (34)$$

The obtained approximations are incompatible now, because the equality of displacements on the sides of the element when it is connected to other elements of the design model is not provided. If in (18) we assume that

$$\boldsymbol{\varphi}_{i3}(\boldsymbol{x}) = \boldsymbol{\lambda}_i(\boldsymbol{x}),\ i=1,2,3,$$

then the resulting system of functions already ensures the convergence of the method, since the equations (17) of the incompatibility criterion will be satisfied if we take the functions (21) of the classic element without rotational degrees of freedom (assuming they are zero) as the system of functions (16). But, as shown by numerical experiments, there is no significant increase in calculation accuracy. Since the element with quasi-rotational degrees of freedom shows good accuracy, then in (18) we take $\boldsymbol{\mu}_i(\boldsymbol{x})$, which are proportional to functions (22), as compatible functions, and $\boldsymbol{\zeta}(\boldsymbol{x})$ – as incompatible ones. We obtain the only possible combination where the equalities of the completeness criterion (15) and the incompatibility criterion (17) are satisfied (If we use functions $\boldsymbol{\zeta}_i(\boldsymbol{x})$, there can be alternative ways of representing functions $\boldsymbol{\varphi}_{i3}(\boldsymbol{x})$, but (35) has shown the best results in the tests):

$$\boldsymbol{\varphi}_{i3}(\boldsymbol{x}) = \frac{1}{3}\left(4\boldsymbol{\chi}_i(\boldsymbol{x}) + \boldsymbol{\zeta}(\boldsymbol{x})\right),\ i=1,2,3. \qquad (35)$$

To increase calculation accuracy, it is reasonable to add five "internal" degrees of freedom with their subsequent condensation. They have corresponding approximations, which satisfy the conditions (19):

$$\boldsymbol{\Psi}_i(\boldsymbol{x}) = \boldsymbol{\Phi}_i(\boldsymbol{x}) - \sum_{k=1}^{3} \boldsymbol{\lambda}_k(\boldsymbol{x}) L_{k3}(\boldsymbol{\Phi}_i(\boldsymbol{x})),$$
$$\boldsymbol{\Phi}_i = \left\{\lambda_{i,v}, -\lambda_{i,u}\right\}^T,\ \boldsymbol{\Psi}_4 = \left\{H,\ 0\right\}^T,\ \boldsymbol{\Psi}_5 = \left\{0,\ H\right\}^T$$
$$H = \xi\eta(1-\xi-\eta),\ i=1.2.3$$

e) Six-node Triangle

Let us consider an element in the local coordinate system, shown in Fig. 1a. After changing the coordinates (20), it is transformed into a triangle shown in Fig. 1b.

We will use fourth-degree polynomials.

Let us determine functions corresponding to the following degrees of freedom:

- rotation angles on the sides:

$$\boldsymbol{\varphi}_{43} = -\frac{2acp(\boldsymbol{x})(e(q-1)+(1-q)\xi+(e-q)\eta)}{a_{13}d(1-d)(e(1-q)+(q-e)d)} \begin{Bmatrix} b \\ c \end{Bmatrix},$$
$$\boldsymbol{\varphi}_{53} = \frac{cp(\boldsymbol{x})(dq+(1-q-d)\xi-q\eta)}{e(1-e)(dq+(1-q-d)e)} \begin{Bmatrix} -2 \\ 0 \end{Bmatrix},$$
$$\boldsymbol{\varphi}_{63} = \frac{2acp(\boldsymbol{x})(ed-d\xi-e\eta)}{a_{23}q(1-q)(ed-dq-e(1-q))} \begin{Bmatrix} a-b \\ c \end{Bmatrix}, \qquad (36)$$

$$p(\boldsymbol{x}) = \xi\eta(1-\xi-\eta)$$

- displacements on the sides:

$$\boldsymbol{\varphi}_{ij}(\boldsymbol{x}) = \boldsymbol{H}_{ij}(\boldsymbol{x}) - \boldsymbol{\varphi}_{i3}(\boldsymbol{x}) L_{i3}(\boldsymbol{H}_{ij}(\boldsymbol{x})), \qquad (37)$$

i=4,5,6, j=1,2,

$$\boldsymbol{H}_{i1} = \begin{Bmatrix} P_{i-3} \\ 0 \end{Bmatrix},\ \boldsymbol{H}_{i2} = \begin{Bmatrix} 0 \\ P_{i-3} \end{Bmatrix},\ P_1 = \frac{(1-\xi-\eta)^2\eta^2}{d^2(1-d)^2},$$

$$P_2 = \frac{\xi^2(1-\xi-\eta)^2}{e^2(1-e)^2},\ P_3 = \frac{\xi^2\eta^2}{q^2(1-q)^2}$$

- rotation angles at the vertices of the triangle, similarly to (35):

$$\boldsymbol{\varphi}_{i3}(\boldsymbol{x}) = \boldsymbol{\Phi}_i(\boldsymbol{x}) - \sum_{j=4}^{6} \boldsymbol{\varphi}_{j3} L_{j3}(\boldsymbol{\Phi}_i(\boldsymbol{x})),$$

$$\boldsymbol{\Phi}_i(\boldsymbol{x}) = \frac{1}{3}\left(4\boldsymbol{\chi}_i(\boldsymbol{x}) + \boldsymbol{\zeta}(\boldsymbol{x})\right), \qquad (38)$$

$$\boldsymbol{\chi}_1 = \frac{1-\xi-\eta}{2}\begin{Bmatrix} c\eta(1-d_1(1-\xi-\eta)\eta) \\ a\xi(1-e_1\xi(1-\xi-\eta)) - \\ \quad b\eta(1-d_1(1-\xi-\eta)\eta) \end{Bmatrix},$$

$$\boldsymbol{\chi}_2 = \frac{\xi}{2}\begin{Bmatrix} -c\xi\eta(1-q_1\xi\eta) \\ -a\xi(1-\xi-\eta)(1-e_1\xi(1-\xi-\eta)) - \\ \quad (a-b)\xi\eta(1-q_1\xi\eta) \end{Bmatrix},$$

$$\boldsymbol{\chi}_3 = \frac{\eta}{2}\begin{Bmatrix} c\xi(1-q_1\xi\eta) - c(1-\xi-\eta)(1-d_1(1-\xi-\eta)\eta) \\ (a-b)\xi(1-q_1\xi\eta) + \\ \quad b(1-\xi-\eta)(1-d_1(1-\xi-\eta)\eta) \end{Bmatrix},$$

$$d_1 = \frac{1}{d(1-d)},\quad e_1 = \frac{1}{e(1-e)},\quad q_1 = \frac{1}{q(1-q)}$$

Compatible functions $\boldsymbol{\chi}_i(\boldsymbol{x})$ are obtained from the condition that the tangential displacement u_τ on the side ij varies quadratically, and the normal displacement u_n varies with θ_i according to the law:

$$\mathrm{u}_n = \ldots + a_{ij}\xi(1-\xi)\left(1 - \frac{\xi(1-\xi)}{a_{ik}(1-a_{ik})}\right)(\theta_j - \theta_i), \qquad (39)$$

k – node on the side ij.
Formula (39) is an extension of the formula (4) taking into account the intermediate node.

$$\boldsymbol{\zeta}(\boldsymbol{x}) = r_1\begin{Bmatrix} c \\ a-b \end{Bmatrix} H_1(\boldsymbol{x}) + r_2\begin{Bmatrix} -c \\ b \end{Bmatrix} H_2(\boldsymbol{x}) + r_3\begin{Bmatrix} 0 \\ -a \end{Bmatrix} H_3(\boldsymbol{x}) \qquad (40)$$

$$H_1(\boldsymbol{x}) = \begin{cases} 0.5\xi\eta((\xi-\eta), & q = 0.5 \\ 2\xi\eta((1-q)\xi - q\eta) & \\ \quad \left((5q\text{-}2)\xi + (3\text{-}5q)\eta\right), & q \neq 0.5 \end{cases}$$

$$H_2(\boldsymbol{x}) = 2\eta(1-\xi-\eta)(-d + d\xi + \eta)$$
$$\left((3\text{-}5d) + (10d\text{-}5)\eta\right)$$

$$H_3(\boldsymbol{x}) = 2\xi(1-\xi-\eta)(e-\xi-e\eta)$$
$$\left((3\text{-}5e) + (10e\text{-}5)\xi\right)$$

The incompatible function $\boldsymbol{\zeta}(\boldsymbol{x})$ in (40) satisfies the equations (19), and the coefficients r_j, j=1,2,3, are found from the system of equations:

$$L_{i3}\boldsymbol{\zeta}(\boldsymbol{x}) = 1,\ i=1,2,3. \qquad (41)$$

- nodal displacements of the element:

$$\boldsymbol{\varphi}_{ij}(\boldsymbol{x}) = \boldsymbol{\Phi}_{ij}(\boldsymbol{x}) - \sum_{k=4}^{6} \boldsymbol{\varphi}_{kj} L_{kj}(\boldsymbol{\Phi}_{ij}), \qquad (42)$$

$$\boldsymbol{\Phi}_{ij}(\boldsymbol{x}) = \boldsymbol{\Psi}_{ij}(\boldsymbol{x}) - \sum_{k=1}^{6} \boldsymbol{\varphi}_{k3}(\boldsymbol{x}) L_{k3}(\boldsymbol{\Psi}_{ij}),$$

i=1,2,3, j=1,2, $\boldsymbol{\Psi}_{ij}(\boldsymbol{x})$ are linear functions (21).
The completeness criterion (15) and the incompatibility criterion (17) are satisfied.
The calculation accuracy can be increased by adding functions corresponding to the internal degrees of freedom:

$$\boldsymbol{\Psi}_i(\boldsymbol{x}) = \boldsymbol{Z}_i(\boldsymbol{x}) - \sum_{j=4}^{6} \boldsymbol{\varphi}_{j3} L_{j3}(\boldsymbol{Z}_i(\boldsymbol{x})),\ i=1,2.$$

$$\boldsymbol{Z}_1 = \{H,\ 0\}^T,\ \boldsymbol{Z}_2 = \{0,\ H\}^T,\ H = \xi\eta(1-\xi-\eta)$$

f) Rectangle with Nodes at Vertices

Let us consider a rectangular finite element in the local coordinate system: a_{12}=a, a_{13}=c. The system of approximating functions of an element will be sought as fifth-degree

polynomials. Assuming $\xi=x/a$, $\eta=y/c$ we will display the element on that shown in Fig. 2b:
Determine the compatible functions $\boldsymbol{\varphi}_{i3}$, i=1,2,3 in (12) with the help of (26) and (27) for ε=–1:

$$\boldsymbol{\varphi}_{13}=\begin{Bmatrix}-c\eta(1-\eta)^2(1-\xi)\\ a\xi(1-\xi)^2(1-\eta)\end{Bmatrix},$$
$$\boldsymbol{\varphi}_{23}=\begin{Bmatrix}-c\eta(1-\eta)^2\xi\\ -a\xi^2(1-\xi)(1-\eta)\end{Bmatrix},$$
$$\boldsymbol{\varphi}_{33}=\begin{Bmatrix}c\eta^2(1-\eta)(1-\xi)\\ a\xi(1-\xi)^2\eta\end{Bmatrix},$$
$$\boldsymbol{\varphi}_{43}=\begin{Bmatrix}c\eta^2(1-\eta)\xi\\ -a\xi^2(1-\xi)\eta\end{Bmatrix} \qquad (43)$$

We adjust the functions of the linear degrees of freedom:

$$\boldsymbol{\varphi}_{11}=\boldsymbol{\Phi}_{11}-\frac{1}{2c}(\boldsymbol{\lambda}_1+\boldsymbol{\lambda}_3),$$
$$\boldsymbol{\varphi}_{12}=\boldsymbol{\Phi}_{12}+\frac{1}{2a}(\boldsymbol{\lambda}_1+\boldsymbol{\lambda}_2),$$
$$\boldsymbol{\varphi}_{21}=\boldsymbol{\Phi}_{21}-\frac{1}{2c}(\boldsymbol{\lambda}_2+\boldsymbol{\lambda}_4),$$
$$\boldsymbol{\varphi}_{22}=\boldsymbol{\Phi}_{22}-\frac{1}{2a}(\boldsymbol{\lambda}_1+\boldsymbol{\lambda}_2),$$
$$\boldsymbol{\varphi}_{31}=\boldsymbol{\Phi}_{31}+\frac{1}{2c}(\boldsymbol{\lambda}_1+\boldsymbol{\lambda}_3),$$
$$\boldsymbol{\varphi}_{32}=\boldsymbol{\Phi}_{32}+\frac{1}{2a}(\boldsymbol{\lambda}_3+\boldsymbol{\lambda}_4),$$
$$\boldsymbol{\varphi}_{41}=\boldsymbol{\Phi}_{41}+\frac{1}{2c}(\boldsymbol{\lambda}_2+\boldsymbol{\lambda}_4),$$
$$\boldsymbol{\varphi}_{42}=\boldsymbol{\Phi}_{42}-\frac{1}{2a}(\boldsymbol{\lambda}_3+\boldsymbol{\lambda}_4), \qquad (44)$$

where: $\boldsymbol{\Phi}_{ij}(\boldsymbol{x})$ is a bilinear system of functions (25);

$$\boldsymbol{\lambda}_1(\boldsymbol{x})=\boldsymbol{\varphi}_{13}(\boldsymbol{x})+\boldsymbol{H}(\boldsymbol{x}),$$
$$\boldsymbol{\lambda}_2(\boldsymbol{x})=\boldsymbol{\varphi}_{23}(\boldsymbol{x})-\boldsymbol{H}(\boldsymbol{x}),$$
$$\boldsymbol{\lambda}_3(\boldsymbol{x})=\boldsymbol{\varphi}_{33}(\boldsymbol{x})-\boldsymbol{H}(\boldsymbol{x}),$$
$$\boldsymbol{\lambda}_4(\boldsymbol{x})=\boldsymbol{\varphi}_{43}(\boldsymbol{x})+\boldsymbol{H}(\boldsymbol{x}), \qquad (45)$$

$$\boldsymbol{H}(\boldsymbol{x})=\frac{5}{4}\begin{Bmatrix}c(1-2\xi)\eta^2(\eta-1)^2\\ -a(1-2\eta)\xi^2(\xi-1)^2\end{Bmatrix}$$

Functions $\boldsymbol{\lambda}_i$, satisfy the equations (19) and ensure the fulfillment of the completeness criterion (15) and the incompatibility criterion (17).

g) Quadrangle

Let us consider a quadrangle shown in Figure 2a and perform the transformation of the coordinate system (28) into a quadrangle shown in Figure 2c. The system of approximating functions of an element will be sought as fourth-degree polynomials in each of the subareas Ω_i of the finite element.
Determine the compatible functions $\boldsymbol{\varphi}_{i3}$, i=1,2,3,4 in (12) with the help of (31) and (32) for ε=–1. Functions $\boldsymbol{\lambda}_i(\boldsymbol{x})$ for adjusting linear approximations can be represented as follows:

$$\boldsymbol{\lambda}_i(\boldsymbol{x})=\boldsymbol{\varphi}_{i3}(\boldsymbol{x})-\sum_{k=1}^{4}r_{ik}\boldsymbol{Z}_k(\boldsymbol{x}) \qquad (46)$$

$$\boldsymbol{Z}_i=\{\gamma_i(\boldsymbol{x}),\ 0\}^T,\quad \boldsymbol{Z}_{i+2}=\{0,\ \gamma_i(\boldsymbol{x})\}^T,\ \text{i=1,2,}$$
$$\gamma_1=\begin{cases}\alpha^2\xi^2\eta^2, & (\xi,\eta)\in\Omega_1\cup\Omega_4\\ -\xi^2\eta^2, & (\xi,\eta)\in\Omega_2\cup\Omega_3\end{cases},$$
$$\gamma_2=\begin{cases}\beta^2\xi^2\eta^2, & (\xi,\eta)\in\Omega_1\cup\Omega_2\\ -\xi^2\eta^2, & (\xi,\eta)\in\Omega_3\cup\Omega_4\end{cases}$$

Coefficients r_{ij} in (46) are obtained as solutions of the systems of equations (19).
Functions corresponding to displacements:

$$\boldsymbol{\varphi}_{ij}(\boldsymbol{x})=\boldsymbol{\Psi}_{ij}(\boldsymbol{x})-\sum_{k=1}^{3}\boldsymbol{\lambda}_k(\boldsymbol{x})L_{k3}(\boldsymbol{\Psi}_{ij}(\boldsymbol{x})), \qquad (47)$$

i=1,2,3,4, j=1,2,

where $\boldsymbol{\Psi}_{ij}(\boldsymbol{x})$ are approximations (30) of an element without rotational degrees of freedom.
The completeness criterion (15) is satisfied for the obtained approximations, since it follows from the properties of functions (31) and (32) that:

$$\sum_{i=1}^{4}\left(\boldsymbol{\varphi}_{i3}(\boldsymbol{x})-\boldsymbol{\lambda}_i(\boldsymbol{x})\right)=\sum_{i,k=1}^{4}s_{ik}\boldsymbol{Z}_k(\boldsymbol{x}) \qquad (48)$$

Functions $\boldsymbol{\zeta}_i(\boldsymbol{x})$ (32) satisfy the equations (19) and, therefore, we obtain a system of equations (19) in (48) for determining the coefficients s_{ik} with zero right-hand side.

h) Eight-node Quadrangle

Let us consider a quadrangle shown in Figure 2a and perform the transformation of the coordinate system (28) into a quadrangle shown in Figure 2c.

$$\omega_z=\frac{1}{2}\left(p_{11}\frac{\partial \mathrm{v}}{\partial\xi}+p_{21}\frac{\partial \mathrm{v}}{\partial\eta}-p_{12}\frac{\partial \mathrm{u}}{\partial\xi}-p_{22}\frac{\partial \mathrm{u}}{\partial\eta}\right) \qquad (49)$$

The system of approximating functions will be sought as incomplete sixth-degree polynomials in the finite element subareas.

Determine functions for the nodes on the sides:

$$\boldsymbol{\varphi}_{i3}=\frac{\zeta_{i-4}(\boldsymbol{x})}{2f_{i-4}}\begin{Bmatrix}n_{yi}\\-n_{xi}\end{Bmatrix},\ i=5,6,7,8, \qquad (50)$$

$$\left\{n_{xi},\ n_{yi}\right\}^T$$

– normal to the side for the node i;

$$f_{i-4}=-(n_{xi}\frac{\partial}{\partial x}+n_{yi}\frac{\partial}{\partial y})\zeta_{i-4}(\boldsymbol{x})|_{\boldsymbol{x}_i}=$$
$$-\Big((n_{xi}r_{11}+n_{yi}r_{12})\frac{\partial}{\partial\xi}+$$
$$(n_{xi}r_{21}+n_{yi}r_{22})\frac{\partial}{\partial\eta})\zeta_{i-4}(\boldsymbol{x})|_{\boldsymbol{x}_i}\Big)$$

$$\zeta_1=\begin{cases}(1-\xi-\eta)\,p(1,A,1,B), & \boldsymbol{x}\in\Omega_1\\ (1-A\xi-\eta)^2(1-A\xi+(2-3B)\eta), & \boldsymbol{x}\in\Omega_2\\ (1-A\xi-B\eta)^3, & \boldsymbol{x}\in\Omega_3\\ (1-\xi-B\eta)^2(1+(2-3A)\xi-B\eta), & \boldsymbol{x}\in\Omega_4\end{cases}$$

$$\zeta_2=\begin{cases}(1-\xi-\eta)^2(1-\xi+(2-3B)\eta), & \boldsymbol{x}\in\Omega_1\\ (1-A\xi-\eta)\,p(A,1,1,B), & \boldsymbol{x}\in\Omega_2\\ (1-A\xi-B\eta)^2(1+(2A-3)\xi-B\eta), & \boldsymbol{x}\in\Omega_3\\ (1-\xi-B\eta)^3, & \boldsymbol{x}\in\Omega_4\end{cases}$$

$$\zeta_3=\begin{cases}(1-\xi-\eta)^3, & \boldsymbol{x}\in\Omega_1\\ (1-A\xi-\eta)^2(1+(2A-3)\xi-\eta), & \boldsymbol{x}\in\Omega_2\\ (1-A\xi-B\eta)\,p(A,1,B,1), & \boldsymbol{x}\in\Omega_3\\ (1-\xi-B\eta)^2(1-\xi+(2B-3)\eta), & \boldsymbol{x}\in\Omega_4\end{cases}$$

$$\zeta_4=\begin{cases}(1-\xi-\eta)^2(1+(2-3A)\xi-\eta), & \boldsymbol{x}\in\Omega_1\\ (1-A\xi-\eta)^3, & \boldsymbol{x}\in\Omega_2\\ (1-A\xi-B\eta)^2(1-A\xi+(2B-3)\eta), & \boldsymbol{x}\in\Omega_3\\ (1-\xi-B\eta)\,p(1,A,B,1), & \boldsymbol{x}\in\Omega_4\end{cases} \qquad (51)$$

$$p(z_1,z_2,z_3,z_4)=1+(z_1-3z_2)\xi+(z_3-3z_4)\eta+$$
$$(3z_2-2z_1)\xi^2++(3z_4-2z_3)\eta^2$$
$$(2z_1z_3-3z_2-3z_4+6z_2z_4)\xi\eta$$

Let us determine functions corresponding to the rotational degrees of freedom in the nodes:

$$\boldsymbol{\varphi}_{i3}(\boldsymbol{x})=\boldsymbol{\Phi}_i(\boldsymbol{x})-\sum_{k=1}^{4}r_{ik}\boldsymbol{\chi}_k(\boldsymbol{x}), \qquad (52)$$

$$\boldsymbol{\Phi}_i(\boldsymbol{x})=\boldsymbol{H}_i(\boldsymbol{x})-\sum_{k=5}^{8}\boldsymbol{\varphi}_{k3}L_{k3}(\boldsymbol{H}_i),\ i=1,2,3,4,$$

where r_{ij} are solutions of the systems of equations (19),

$$\boldsymbol{H}_i(\boldsymbol{x})=\boldsymbol{\psi}_{k3}(\boldsymbol{x})T_i(\boldsymbol{x}),$$

$\boldsymbol{\psi}_{k3}(\boldsymbol{x})$ – are compatible functions of a quadrangular element with piecewise polynomial approximation (29-31) for ε=–1;

$$T_1=P_{781},\ T_2=P_{582},\ T_3=P_{673},\ T_4=P_{564}, \qquad (53)$$

$$P_{ijk}(\boldsymbol{x})=\frac{(\xi-\xi_i)(\eta_j-\eta_i)-(\eta-\eta_i)(\xi_j-\xi_i)}{(\xi_k-\xi_i)(\eta_j-\eta_i)-(\eta_k-\eta_i)(\xi_j-\xi_i)}$$

$$\boldsymbol{\chi}_i(\boldsymbol{x})=\boldsymbol{Z}_i-\sum_{j=1}^{4}\sum_{k=5}^{8}\boldsymbol{\varphi}_{kj}L_{kj}(\boldsymbol{Z}_i) \qquad (54)$$

$$\boldsymbol{Z}_i=\left\{\gamma_i(\boldsymbol{x}),\ 0\right\}^T,\ \boldsymbol{Z}_{i+2}=\left\{0,\ \gamma_i(\boldsymbol{x})\right\}^T,\ i=1,2,$$

$$\gamma_1=\xi^3\eta^3\begin{cases}\alpha^3\beta^3, \boldsymbol{x}\in\Omega_1\\ \beta^3, \quad \boldsymbol{x}\in\Omega_2\\ -1, \quad \boldsymbol{x}\in\Omega_3\\ -\alpha^3, \ \boldsymbol{x}\in\Omega_4\end{cases},$$

$$\gamma_2=\xi^3\eta^3\begin{cases}\alpha^3\beta^3, \ \boldsymbol{x}\in\Omega_1\\ -\beta^3, \quad \boldsymbol{x}\in\Omega_2\\ -1, \quad \boldsymbol{x}\in\Omega_3\\ \alpha^3, \quad \boldsymbol{x}\in\Omega_4\end{cases}$$

Adjust functions (29), ψ_i , i=1÷8:

$$\chi_i(\boldsymbol{x})=\psi_i(\boldsymbol{x})-\sum_{m=5}^{8}\psi_i(\boldsymbol{x}_m)\chi_m(\boldsymbol{x}),, \qquad (55)$$

$$\chi_k(\boldsymbol{x})=\frac{\psi_k(\boldsymbol{x})}{\psi_k(\boldsymbol{x}_k)}$$

i=1,2,3,4, k=5,6,7,8.

Functions corresponding to displacements are obtained using (55):

$$\boldsymbol{\varphi}_{ij}(\boldsymbol{x})=\boldsymbol{\Psi}_{ij}(\boldsymbol{x})-\sum_{k=1}^{8}\boldsymbol{\varphi}_{k3}(\boldsymbol{x})L_{k3}(\boldsymbol{\Psi}_{ij}), \qquad (56)$$

$$\boldsymbol{\Psi}_{i1}(\boldsymbol{x})=\begin{Bmatrix}\chi_i\\0\end{Bmatrix}, \ \boldsymbol{\Psi}_{i2}(\boldsymbol{x})=\begin{Bmatrix}0\\\chi_i\end{Bmatrix}, \ \ i=1\div8, j=1,2$$

The obtained system of functions satisfies the completeness criterion (15) and the incompatibility criterion (17).

2.3. Compatible Elements (ω_z)

i) Triangle with Nodes at Vertices

Let us consider a triangle shown in Fig. 1a, and perform the transformation of the coordinate system (57) into a triangle shown in Fig. 1c, where point A is the intersection point of the medians of the triangle:

$$\begin{cases}\xi=p_{11}x+p_{12}y-1\\ \eta=p_{21}x+p_{22}y-1\end{cases} \qquad (57)$$

$$p_{11}=\frac{2}{a}, \ p_{12}=\frac{a-2b}{ac}, \ \ p_{21}=\frac{1}{a}, \ p_{22}=\frac{2a-b}{ac}$$

Let us write the functions $\boldsymbol{\lambda}_i(\boldsymbol{x})$, i=1,2,3, which are second-degree polynomials in each of the subareas, are zero on the sides of the triangle, continuous within Ω and satisfy the conditions (14). We obtain the unique solution:

$$\boldsymbol{\lambda}_1(\boldsymbol{x})=\frac{2}{9}\begin{Bmatrix}c\\-a-b\end{Bmatrix}\gamma_1(\boldsymbol{x}), \quad \boldsymbol{\lambda}_3(\boldsymbol{x})=\frac{2}{9}\begin{Bmatrix}-2c\\2b-a\end{Bmatrix}\gamma_3(\boldsymbol{x})$$

$$\boldsymbol{\lambda}_2(\boldsymbol{x})=\frac{2}{9}\begin{Bmatrix}c\\2a-b\end{Bmatrix}\gamma_2(\boldsymbol{x}), \qquad (58)$$

$$\zeta=\begin{cases}1-\xi-\eta, & \boldsymbol{x}\in\Omega_1 \quad \gamma_1(\boldsymbol{x})=(1-\xi-\eta)\zeta,\\ 1+2\xi-\eta, & \boldsymbol{x}\in\Omega_2, \quad \gamma_2(\boldsymbol{x})=(1-\xi+2\eta)\zeta,\\ 1-\xi+2\eta, & \boldsymbol{x}\in\Omega_3 \quad \gamma_3(\boldsymbol{x})=(1+2\xi-\eta)\zeta,\end{cases}$$

Functions $\boldsymbol{\lambda}_i$, i=1,2,3 have *discontinuities* ω_z at the boundaries Ω_i (sides of connected elements, segments of medians), but $\omega_z(\boldsymbol{\lambda}_i(\boldsymbol{x}))$ are *continuous* at the nodes of the element.

Compatible functions corresponding to the rotational degrees of freedom and satisfying the conditions (14), similarly to (35), can be represented as follows:

$$\boldsymbol{\varphi}_{i3}(\boldsymbol{x})=\frac{1}{3}\left(4\boldsymbol{\chi}_i(\boldsymbol{x})+\boldsymbol{\zeta}(\boldsymbol{x})\right), \qquad (59)$$

$$\boldsymbol{\zeta}(\boldsymbol{x})=\boldsymbol{\lambda}_1(\boldsymbol{x})+\boldsymbol{\lambda}_2(\boldsymbol{x})+\boldsymbol{\lambda}_3(\boldsymbol{x})$$

where $\boldsymbol{\chi}_i$ are functions (22) in the coordinate system (57).

The functions corresponding to displacements are obtained by substituting the functions $\boldsymbol{\zeta}_i(\boldsymbol{x})$ from (59) and linear functions into (34):

$$\psi_1(\boldsymbol{x})=\frac{1}{3}(1-\xi-\eta), \ \psi_2(\boldsymbol{x})=\frac{1}{3}(1+2\xi-\eta),$$

$$\psi_3(\boldsymbol{x})=\frac{1}{3}(1-\xi+2\eta)$$

The calculation accuracy can be increased by adding functions equal to zero on the sides of the element as those corresponding to internal degrees of freedom:

$$\boldsymbol{\psi}_1(\boldsymbol{x})=\{R,\ 0\}^T,\quad \boldsymbol{\psi}_2(\boldsymbol{x})=\{0,\ R\}^T,$$
$$R(\boldsymbol{x})=\begin{cases}(1-\xi-\eta)^2, & \boldsymbol{x}\in\Omega_1\\ (1+2\xi-\eta)^2, & \boldsymbol{x}\in\Omega_2\\ (1-\xi+2\eta)^2, & \boldsymbol{x}\in\Omega_3\end{cases}$$

j) Six-node Triangle

Let us consider a triangle shown in Figure 1a, and perform the transformation of the coordinate system (57) into a triangle shown in Fig. 1c. The functions are sought as third-degree polynomials in each of the subareas.

Functions corresponding to the rotational degrees of freedom at the nodes are given by adjusting (58) (functions (36) can be applied, which will result in fourth-degree polynomials):

$$\boldsymbol{\varphi}_{i3}(\boldsymbol{x})=\boldsymbol{\lambda}_i(\boldsymbol{x})-\sum_{k=4}^{6}\boldsymbol{\varphi}_{i3}(\boldsymbol{x})L_{k3}(\boldsymbol{\lambda}_i(\boldsymbol{x})),\ i=1,2,3,\quad (60)$$
$$\boldsymbol{\varphi}_{43}(\boldsymbol{x})=\frac{\mathrm{c}}{3\eta_4(\xi_4-\eta_4)}\begin{Bmatrix}-1\\0\end{Bmatrix}H_1,$$
$$\boldsymbol{\varphi}_{53}(\boldsymbol{x})\frac{a\mathrm{c}}{3a_{13}^2\xi_5(\xi_5-\eta_5)}\begin{Bmatrix}b\\c\end{Bmatrix}H_2,$$
$$\boldsymbol{\varphi}_{63}(\boldsymbol{x})\frac{a\mathrm{c}}{3a_{23}^2\xi_6\eta_6}\begin{Bmatrix}a-b\\c\end{Bmatrix}H_3$$
$$H_1=\begin{cases}\eta(\eta-\xi)(1-\xi+2\eta), & \boldsymbol{x}\in\Omega_3\\ 0, & \boldsymbol{x}\in\Omega_1\cup\Omega_2\end{cases},$$
$$H_2=\begin{cases}\xi(\xi-\eta)(1+2\xi-\eta), & \boldsymbol{x}\in\Omega_2\\ 0, & \boldsymbol{x}\in\Omega_1\cup\Omega_3\end{cases},$$
$$H_3=\begin{cases}\xi\eta(1-\xi-\eta), & \boldsymbol{x}\in\Omega_1\\ 0, & \boldsymbol{x}\in\Omega_2\cup\Omega_3\end{cases}$$

Functions corresponding to displacements are obtained from approximations of a classic element $\boldsymbol{\psi}_{ij}(\boldsymbol{x})$ without rotational degrees of freedom:

$$\boldsymbol{\varphi}_{ij}(\boldsymbol{x})=\boldsymbol{\psi}_{ij}(\boldsymbol{x})-\sum_{k=1}^{6}\boldsymbol{\varphi}_{k3}(\boldsymbol{x})L_{k3}(\boldsymbol{\psi}_{ij}(\boldsymbol{x})),\quad (61)$$

$i=1\div6$, $j=1,2$

The calculation accuracy can be increased by adding functions equal to zero on the sides of the element as those corresponding to eleven internal degrees of freedom:

$$\boldsymbol{\Psi}_i(\boldsymbol{x})=\boldsymbol{Z}_i(\boldsymbol{x})-\sum_{k=4}^{6}\boldsymbol{\varphi}_{i3}(\boldsymbol{x})L_{k3}(\boldsymbol{Z}_i(\boldsymbol{x})),\ i=1,2,3,$$
$$\boldsymbol{Z}_i(\boldsymbol{x})=\{\varphi_{i+3,3,v},\ -\varphi_{i+3,3,u}\}^T,$$
$$\boldsymbol{\Psi}_4=\begin{Bmatrix}R\\0\end{Bmatrix},\ \boldsymbol{\Psi}_5=\begin{Bmatrix}0\\R\end{Bmatrix},\ \boldsymbol{\Psi}_6(\boldsymbol{x})=\begin{Bmatrix}R_1\\0\end{Bmatrix},\ \boldsymbol{\Psi}_7(\boldsymbol{x})=\begin{Bmatrix}0\\R_1\end{Bmatrix}$$
$$\boldsymbol{\Psi}_8=\xi\boldsymbol{\Psi}_4,\ \boldsymbol{\Psi}_9=\xi\boldsymbol{\Psi}_5,\ \boldsymbol{\Psi}_{10}=\eta\boldsymbol{\Psi}_4,\ \boldsymbol{\Psi}_{11}=\eta\boldsymbol{\Psi}_5$$
$$R_1(\boldsymbol{x})=\begin{cases}0, & \boldsymbol{x}\in\Omega_1\\ \xi(1+2\xi-\eta)(1-\eta), & \boldsymbol{x}\in\Omega_2\\ \eta(1-\xi+2\eta)(1-\xi), & \boldsymbol{x}\in\Omega_3\end{cases}$$

k) Quadrangle with Nodes at Vertices

Let us consider a convex quadrangle shown in Figure 2a and perform the transformation of the coordinate system (28) into a quadrangle shown in Figure 2c.

The functions are sought as second-degree polynomials in each of the subareas.

Let us write the functions $\boldsymbol{\lambda}_i(\boldsymbol{x})$, i=1,2,3,4, which are second-degree polynomials in each of the subareas, are zero on the sides of the quadrangle, continuous within Ω and satisfy the conditions (14). We obtain the unique solution:

$$\boldsymbol{\lambda}_1(\boldsymbol{x})=\frac{2}{p}\begin{Bmatrix}p_{11}\\p_{12}\end{Bmatrix}\gamma_1,\quad \boldsymbol{\lambda}_2(\boldsymbol{x})=-\frac{2}{p}\begin{Bmatrix}p_{21}\\p_{22}\end{Bmatrix}\gamma_2,$$
$$\boldsymbol{\lambda}_3(\boldsymbol{x})=\frac{2}{p}\begin{Bmatrix}p_{21}\\p_{22}\end{Bmatrix}\gamma_3,\quad \boldsymbol{\lambda}_4(\boldsymbol{x})=-\frac{2}{p}\begin{Bmatrix}p_{11}\\p_{12}\end{Bmatrix}\gamma_4\quad (62)$$

$$p=p_{11}p_{22}-p_{12}p_{21},$$
$$\gamma_1=\begin{cases}\eta(1-A\xi-B\eta), & \boldsymbol{x}\in\Omega_3\\ \eta(1-\xi-B\eta), & \boldsymbol{x}\in\Omega_4\\ 0, & \boldsymbol{x}\in\Omega_1\cup\Omega_2\end{cases}$$
$$\gamma_2=\begin{cases}\xi(1-\xi-\eta), & \boldsymbol{x}\in\Omega_1\\ \xi(1-\xi-B\eta), & \boldsymbol{x}\in\Omega_4\\ 0, & \boldsymbol{x}\in\Omega_2\cup\Omega_3\end{cases}$$
$$\gamma_3=\begin{cases}\eta(1-A\xi-\eta), & \boldsymbol{x}\in\Omega_2\\ \eta(1-A\xi-B\eta), & \boldsymbol{x}\in\Omega_3\\ 0, & \boldsymbol{x}\in\Omega_1\cup\Omega_4\end{cases}$$

$$\gamma_4 = \begin{cases} \xi(1-\xi-\eta), & \boldsymbol{x} \in \Omega_1 \\ \xi(1-A\xi-\eta), & \boldsymbol{x} \in \Omega_2 \\ 0, & \boldsymbol{x} \in \Omega_3 \bigcup \Omega_4 \end{cases}$$

Similarly to a triangular element, functions $\boldsymbol{\lambda}_i$, i=1,2,3,4 have *discontinuities* ω_z at the boundaries Ω_i (sides of connected elements, segments of diagonals), but $\omega_z(\boldsymbol{\lambda}_i(\boldsymbol{x}))$ is *continuous* at its nodes.

Compatible functions which correspond to rotational degrees of freedom, preserve equalities (15) and satisfy the equations of the incompatibility criterion (17) are given in the following form, taking into account the experience of creating triangular elements:

$$\boldsymbol{\varphi}_{i3}(\boldsymbol{x}) = \frac{1}{3}(4\boldsymbol{\chi}_i(\boldsymbol{x}) - \sum_{j=1}^{4} \kappa(i,j)\boldsymbol{\lambda}_j(\boldsymbol{x})), \qquad (63)$$

$$\kappa(i,j) = \begin{cases} 1, & ij - side \\ 0, & ij - diagonal \end{cases}$$

where $\boldsymbol{\chi}_i(\boldsymbol{x})$, i=1,2,3,4 are functions (31).

Functions corresponding to displacements are obtained from approximations (29) of an element without rotational degrees of freedom by adjusting them with the help of functions $\boldsymbol{\lambda}_i(\boldsymbol{x})$ to satisfy the conditions (14):

$$\boldsymbol{\varphi}_{ij}(\boldsymbol{x}) = \boldsymbol{\psi}_{ij}(\boldsymbol{x}) - \sum_{k=1}^{4} \boldsymbol{\lambda}_k(\boldsymbol{x}) L_{k3}(\boldsymbol{\psi}_{ij}), \qquad (64)$$

The calculation accuracy can be increased by adding functions equal to zero on the sides of the element as those corresponding to internal degrees of freedom:

$$\boldsymbol{\Psi}_4(\boldsymbol{x}) = \{R, 0\}^T, \ \boldsymbol{\Psi}_5(\boldsymbol{x}) = \{0, R\}^T, \qquad (65)$$

$$R(\boldsymbol{x}) = \begin{cases} (1-\xi-\eta)^2, & \boldsymbol{x} \in \Omega_1 \\ (1-A\xi-\eta)^2, & \boldsymbol{x} \in \Omega_2 \\ (1-A\xi-B\eta)^2, & \boldsymbol{x} \in \Omega_3 \\ (1-\xi-B\eta)^2 & \boldsymbol{x} \in \Omega_4 \end{cases}$$

l) Eight-node Quadrangle

Let us consider a convex quadrangle shown in Fig. 2a and perform the transformation of the coordinate system (28) into a quadrangle shown in Fig. 2c. The functions are sought as third-degree polynomials in each of the subareas.

Functions corresponding to the rotational degrees of freedom can be given as follows:

$$\boldsymbol{\varphi}_{i3}(\boldsymbol{x}) = \boldsymbol{\lambda}_i(\boldsymbol{x}) - \sum_{k=5}^{8} \boldsymbol{\varphi}_{k3}(\boldsymbol{x}) L_{k3}(\boldsymbol{\lambda}_i(\boldsymbol{x})), \qquad (66)$$

$$\boldsymbol{\varphi}_{k3}(\boldsymbol{x}) = \boldsymbol{\psi}_{k3}(\boldsymbol{x}), \ i=1,2,3,4, \ k=5,6,7,8,$$

where $\boldsymbol{\psi}_{i3}(\boldsymbol{x})$ are functions (50), $\boldsymbol{\lambda}_i(\boldsymbol{x})$ are functions (62).

Functions corresponding to displacements are obtained according to formula (56) by substituting functions (66).

The calculation accuracy can be increased by adding functions equal to zero on the sides of the element as those corresponding to eleven internal degrees of freedom functions (65).

2.4. Accuracy of Elements

The considered finite elements, except for the isoparametric ones, use polynomial or piecewise polynomial approximations of the displacement field over the entire area of the element.

Equalities of the completeness criterion (15) are satisfied for all elements including isoparametric ones. Let us add the equalities of the completeness criterion of the 2-nd order to them:

$$\sum_{i=1}^{N} x_i^2 \boldsymbol{\varphi}_{i1}(\boldsymbol{x}) \equiv \begin{Bmatrix} x^2 \\ 0 \end{Bmatrix}, \ \sum_{i=1}^{N} y_i^2 \boldsymbol{\varphi}_{i2}^r(\boldsymbol{x}) \equiv \begin{Bmatrix} 0 \\ y^2 \end{Bmatrix}$$

$$\sum_{i=1}^{N} x_i (y_i \boldsymbol{\varphi}_{i1}^r(\boldsymbol{x}) - \frac{1}{2}\boldsymbol{\varphi}_{i3}^r(\boldsymbol{x})) \equiv \begin{Bmatrix} xy \\ 0 \end{Bmatrix},$$

$$\sum_{i=1}^{N} y_i (y_i \boldsymbol{\varphi}_{i1}^r(\boldsymbol{x}) - \boldsymbol{\varphi}_{i3}^r(\boldsymbol{x})) \equiv \begin{Bmatrix} y^2 \\ 0 \end{Bmatrix},$$

$$\sum_{i=1}^{N} x_i (x_i \boldsymbol{\varphi}_{i2}^r(\boldsymbol{x}) + \boldsymbol{\varphi}_{i3}^r(\boldsymbol{x})) \equiv \begin{Bmatrix} 0 \\ x^2 \end{Bmatrix},$$

$$\sum_{i=1}^{N} y_i (x_i \boldsymbol{\varphi}_{i2}^r(\boldsymbol{x}) + \frac{1}{2}\boldsymbol{\varphi}_{i3}^r(\boldsymbol{x})) \equiv \begin{Bmatrix} 0 \\ xy \end{Bmatrix}, \qquad (67)$$

They are satisfied only for compatible 6-node triangular and 8-node quadrangular elements whose functions are sought as second-degree polynomials. Despite a rather large number of degrees of freedom, the equalities (67) are *not satisfied* for elements with quasi-rotational degrees of freedom and all incompatible elements.

Considering that the equalities of the incompatibility criterion (17) are satisfied for all incompatible elements, we obtain the following minimum estimates of the order of the convergence rate according to [15] for regular partitions with sufficiently smooth boundary in the L_2 norm for elements:

- ***a-i, k*** – the first one in stresses and the second one in displacements;
- ***j, l*** (high-precision compatible elements) – the second one in stresses and the third one in displacements.

3. TESTS

All tests for elements with quasi-rotational degrees of freedom were performed with the value ε=0.001. Since the values of displacements and stresses calculated for these elements according to the hypothesis (4), and hypothesis (5) for the given ε *differ only in the fourth significant digit*, and only on the coarsest mesh, they are not provided.

All the approximations considered in this paper and corresponding to the "internal" degrees of freedom of the elements are applied.

The loads specified as uniformly distributed, trapezoidal and *parabolic* were reduced to nodal ones taking into account the condensation of "internal" degrees of freedom.

All calculations were performed in SCAD, which is a part of SCAD Office®.

3.1. Patch Tests

Patch tests [21] are performed in order to check whether the equalities of the completeness criterion (15) are satisfied for all considered elements:

- stiffness matrices of all considered finite elements each have three eigenvectors corresponding to their ***displacement as rigid bodies***;
- the results for plates under constant stresses were obtained with an accuracy up to a computational error.

These tests serve only as a correctness criterion of the program code.

3.2. Narrow Rectangular Plate

The plate of rectangular section shown in Fig. 3 is subjected to a trapezoidal load applied at its ends P=±2*kEy,* E=100kPa, ν=0, h=1m, a=10m, b=1m. Coefficient k=0.06 results in unit moments at the ends of the plate, when it is considered as a bar.

The problem has an analytical solution, known from the theory of elasticity:

$$u=-\frac{2}{b}kxy,\quad v=\frac{1}{b}k\left(y^2+x^2-\frac{1}{4}a^2\right) \qquad (68)$$

The design models shown in Fig. 4 are taken from [7], where this problem was considered. Table 1 contains calculated vertical displacements at the point A(0,5), stresses σ_x at the point B(0,–5) and rotation angles ω at the point E(1.6(6),0). The following analytical solutions are obtained from (68):

$$v_A=-1.5\text{m},\ \sigma_{x,B}=6\text{kPa},\ \omega_E=0.4\text{rad}.$$

If the given plate is considered as a bar, then after applying a pair of moments at its ends

$$M_y=\pm 2kEJ_y/\text{h},\ J_y=\text{hb}^3/12$$

(moment of inertia of the plate section), we obtain the same values of vertical deflection and rotation angle using rod theory.

A loading statically equivalent to the given load was considered to study moment loads, when the moments M_y are specified in the nodes C(-5,0) and D(5,0). Table 2 shows the results of experiments.

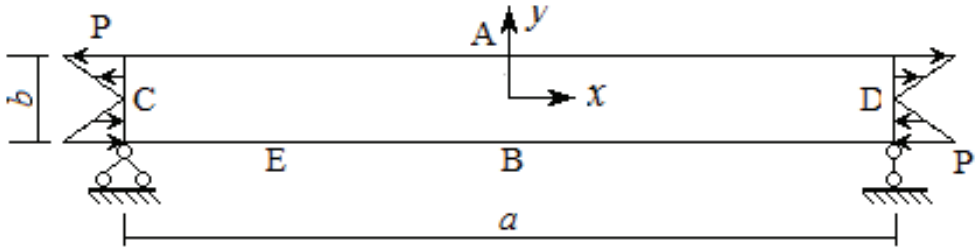

Figure 3. Narrow plate.

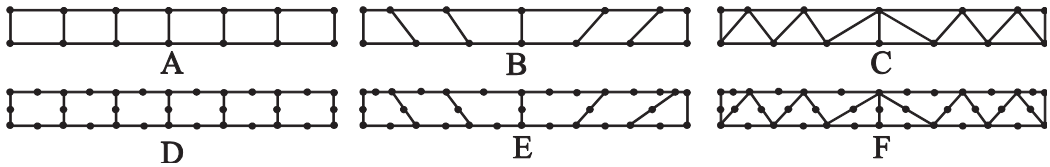

Figure 4. Design models 1x6 for a narrow rectangular plate.

Table 1. Displacements, stresses and rotation angles in a narrow plate.

Mesh type	Element	Displacements w_A (m)				Stresses σ_B (kPa)				Rotation angles ω_E (rad)			
		Mesh				Mesh				Mesh			
		1x6	2x12	4x24	8x48	1x6	2x12	4x24	8x48	1x6	2x12	4x24	8x48
A	*b, c*	-1.5				6				0.4			
	f	-1.231	-1.422	-1.480	-1.496	4.874	5.673	5.915	5.978	0.3255	0.3783	0.3943	0.3986
	g	-1.203	-1.412	-1.478	-1.495	4.775	5.639	5.905	5.976	0.3199	0.3761	0.3937	0.3984
	k	-0.923	-1.295	-1.442	-1.485	3.052	4.743	5.529	5.817	0.2430	0.3450	0.3846	0.3960
B	*b*	-1.298	-1.458	-1.490	-1.497	5.711	6.020	5.998	5.999	0.2945	0.3771	0.3933	0.3961
	c	-1.318	-1.458	-1.490	-1.497	5.686	6.027	6.001	6	0.3234	0.3838	0.3943	0.3964
	g	-0.777	-1.222	-1.418	-1.479	3.267	5.241	5.805	5.951	0.2005	0.3198	0.3758	0.3936
	k	-0.766	-1.200	-1.410	-1.476	2.332	4.088	5.280	5.747	0.2011	0.3193	0.3758	0.3936
C	*a*	-0.858	-1.261	-1.432	-1.482	3.318	5.026	5.741	5.939	0.2079	0.3750	**0.4570**	**0.4780**
	d	-0.920	-1.291	-1.440	-1.484	4..814	6.096	6.252	6.171	0.2323	0.3389	0.3823	0.3952
	i	-0.684	-1.118	-1.372	-1.464	1.779	3.412	4.894	5.635	0.1793	0.2991	0.3667	0.3908
D	*h*	-1.512	-1.502	-1.5		6.038	6.009	6.002	6.001	0.4012	0.3993	0.3998	0.4
	l	-1.5				6				0.4			
E	*h*	-1.511	-1.502	-1.5	-1.5	6.246	6.072	6.019	6.005	0.3934	0.3958	0.3983	0.3993
	l	-1.5				6				0.4			
F	*e*	-1.367	-1.461	-1.490	-1.497	5.318	5.754	5.914	5.970	0.3601	0.3897	0.3974	0.3993
	j	-1.5				6				0.4			

The obtained results slightly differ from those given in Table 2 only for elements with the degrees of freedom ω_z.

Numerical experiments show that the obtained rotation angles for the element with quasi-rotational degrees of freedom are *incorrect*.

3.3. Cantilever Plate under Simple Bending

Let us consider a plate shown in Figure 5: E=3e7kPa, ν=0.25, h=1m, *a*=48m, *b*=12m. The plate is subjected to the following loads:

- on the side x=*a* :
  f_y=–6ry(*b*-y) – parabolic load;
- on the side x=0 : f_x=6r*a*(*b*-2y);
  f_y=6ry(*b*–y), r=f/b^3/E, *f*=40kN.

Table 2. Displacements, stresses and rotation angles in a narrow plate (loaded by a concentrated moment).

Mesh type	Element	Displacements w_A (m)				Stresses σ_B (kPa)				Rotation angles ω_E (rad)			
		Mesh				Mesh				Mesh			
		1x6	2x12	4x24	8x48	1x6	2x12	4x24	8x48	1x6	2x12	4x24	8x48
A	*b*	-1.499	-1.467	-1.457	-1.453	5.996	5.998	5.997	5.991	**0.6877**	**1.5776**	**5.0046**	**18.805**
	c	-1.499	-1.474	-1.464	-1.454	5.996	5.998	5.997	5.991	**0.6877**	**1.5516**	**5.0064**	**18.803**
	f	-1.286	-1.397	-1.449	-1.470	4.877	5.673	5.915	5.978	0.3178	0.3784	0.3943	0.3986
	g	-1.255	-1.403	-1.452	-1.470	4.775	5.639	5.905	5.976	0.3170	0.3749	0.3937	0.3984
	k	-0.938	-1.291	-1.431	-1.472	3.053	4.743	5.529	5.817	0.2409	0.3454	0.3846	0.3960
B	*b*	-1.225	-1.393	-1.456	-1.442	5.801	6.424	6.446	6.413	**0.5241**	**0.9224**	**2.8121**	**10.096**
	c	-1.295	-1.419	-1.441	-1.443	5.803	6.392	6.428	6.408	**0.6074**	**1.2582**	**3.103**	**10.373**
	g	-0.796	-1.208	-1.390	-1.455	3.264	5.241	5.805	5.951	0.1970	0.3207	0.3758	0.3936
	k	-0.780	-1.194	-1.396	-1.461	2.336	4.088	5.280	5.747	0.1999	0.3186	0.3758	0.3936
C	*a*	-1.029	-1.502	**-1.700**	**-1.747**	4.305	**6.959**	**8.027**	**8.017**	**0.5514**	**0.6701**	**2.4418**	**9.1624**
	d	-0.916	-1.279	-1.423	-1.467	4..801	6.097	6.252	6.171	0.2429	0.3447	0.3828	0.3952
	i	-0.697	-1.113	-1.359	-1.451	1.781	3.412	4.894	5.635	0.1785	0.2983	0.3668	0.3908
D	*h*	-1.528	-1.494	-1.494	-1.490	6.072	6.013	6.002	6.001	0.3897	0.4034	0.3953	0.3991
	l	-1.511	-1.496	-1.487	-1.483	6.003	6			0.3991	0.3996	0.4	
E	*h*	-1.521	-1.493	-1.495	-1.489	6.295	6.069	6.019	6.005	0.3703	0.4088	0.3976	0.3987
	l	-1.504	-1.490	-1.484	-1.484	5.998	6			0.3993	0.3974	0.4	
F	*e*	-1.372	-1.477	-1.490	-1.488	5.300	5.754	5.914	5.970	0.3788	0.3917	0.3974	0.3993
	j	-1.514	-1.519	-1.485	-1.482	6.001	6			0.3983	0.3994	0.3999	0.4

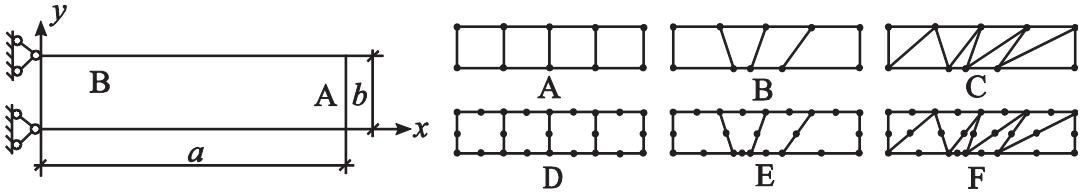

Figure 5. Cantilever plate and its design models.

This problem has an analytical solution:

$$\begin{aligned} \mathrm{u} &= r(3(b-2y)(x-a)^2-(\nu+2)(3by^2- \\ &\quad 2y^3)(6a^2+(\nu+2)b^2)y-3ba^2) \\ \mathrm{v} &= r(-6\nu(by-\mathrm{y}^2)(x-a)+ \\ &\quad 2(x-a)^2-(6a^2+(\nu+2)b^2)x+2a^3) \end{aligned} \qquad (69)$$

The load on the side x=0 was ignored in many studies. In the case of the third degree of freedom it is an approximation even when there no additional nodes on the side of the cantilever. The design models shown in Figure 5 are taken from [2], where this problem was considered. Table 3 contains calculated vertical displacements at the point A(48,6) and stresses σ_x at the point B(12,12). The following analytical solution is obtained from (69): w_A=–0.353(3)m, $\sigma_{x,B}$=60kPa.
0.353(3)m, $\sigma_{x,B}$=60kPa.

3.4. Cook's Problem

Let us consider a wedge with a clamped left edge shown in Figure 6. A uniformly distributed load P is applied to its right edge. Following [4] we take:

$$E = 1\mathrm{Pa},\ \nu = 0.3(3),\ h = 1\mathrm{m},$$
$$P = 0.0625\ \mathrm{N/m},\ u|_{x=0}=0,\ v|_{x=0}=0.$$

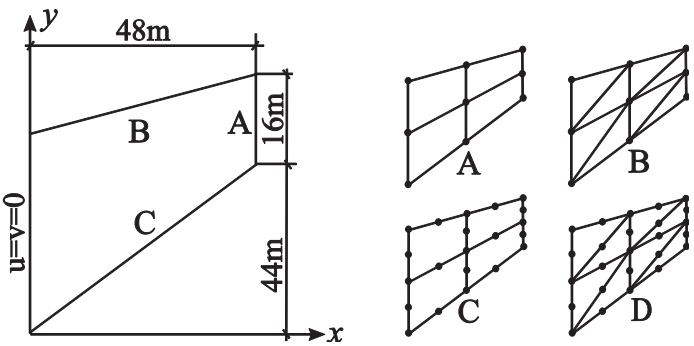

Figure 6. Wedge and its design models.

Table 3. Displacements and stresses in a cantilever plate.

Mesh type	Element	Displacements w_A (m)				Stresses σ_B (kPa)			
		Mesh				Mesh			
		1x4	2x8	4x16	8x32	1x4	2x8	4x16	8x32
A	*b*	-0.3283	-0.3456	-0.3511	-0.3527	59.988	60.998	60.746	60.438
	c	-0.3283	-0.3458	-0.3512	-0.3527	59.988	60.980	60.746	60.437
	f	-0.3541	-0.3583	-0.3586	-0.3572	64.969	61.874	61.028	60.509
	g	-0.3480	-0.3556	-0.3572	-0.3564	63.811	61.823	60.990	60.500
	k	-0.2742	-0.3264	-0.3451	-0.3510	43.205	54.035	57.923	59.226
B	*b*	-0.3342	-0.3465	-0.3513	-0.3527	61.512	61.304	60.945	60.501
	c	-0.3271	-0.3462	-0.3513	-0.3528	59.743	61.140	60.934	60.501
	g	-0.3227	-0.3487	-0.3544	-0.3553	61.805	62.292	61.366	60.725
	k	-0.2614	-0.3216	-0.3434	-0.3504	39.607	52.825	57.497	59.064
C	*a*	-0.2471	-0.3179	-0.3427	-0.3503	36.867	50.599	56.499	58.611
	d	-0.2673	-0.3236	-0.3440	-0.3505	44.407	52.306	57.177	59.052
	i	-0.2141	-0.2902	-0.3297	-0.3457	35.949	48.270	55.999	58.521
D	*h*	-0.3567	-0.3522	-0.3521	-0.3525	64.896	61.840	60.458	60.128
	l	-0.3540	-0.3534	-0.3533	-0.3533	60.004	60		
E	*h*	-0.3585	-0.3529	-0.3522	-0.3525	63.849	61.159	60.288	60.092
	l	-0.3533				59.328	59.804	59.960	59.991
F	*e*	-0.3398	-0.3488	-0.3519	-0.3529	41.195	52.981	57.554	58.844
	j	-0.3470	-0.3523	-0.3532	-0.3533	62.438	60.555	60.090	60.017

A statically equivalent stress was also considered when uniformly distributed moments were applied at the ends of the plate and reduced to a nodal load using the formula (8).

No analytical solution is known for this problem. Stable numerical solution with an accuracy of up to 6 significant digits, obtained with various finite elements and mesh refinement up to 1024x1024 (3149825 nodes, 2^{20} elements):

- vertical displacement w_A=–23.9677m,
- principal stresses $\sigma_{1,B}$=0.203525 Pa and $\sigma_{3,C}$=–0.23687 Pa.

Table 4 shows the results of experiments.

Some papers assume ν=0.3. The values are slightly different in this case:

w_A=–23.9119m, $\sigma_{1,B}$=0.20353Pa
and $\sigma_{3,C}$=–0.23692Pa.

Table 4. Displacements and principal stresses in Cook's problem.

Mesh type	Element	Displacements w_A (m)				Pr. stresses $\sigma_{1,B}$ (kPa)				Pr. stresses $\sigma_{3,C}$ (kPa)			
		Mesh				Mesh				Mesh			
		2x2	4x4	8x8	16x16	2x2	4x4	8x8	16x16	2x2	4x4	8x8	16x16
A	*b*	-21.66	-23.23	-23.78	-23.92	0.1774	0.1977	0.2009	0.2032	-0.1730	-0.2197	-0.2322	-0.2354
	c	-21.56	-23.22	-23.78	-23.92	0.1747	0.1977	0.2007	0.2032	-0.1711	-0.2193	-0.2322	-0.2354
	g	-17.26	-21.92	-23.37	-23.79	0.1777	0.2013	0.2039	0.2049	-0.1760	-0.2279	-0.2388	-0.2395
	k	-17.55	-21.53	-23.13	-23.69	0.1430	0.1769	0.1953	0.2013	-0.1470	-0.1982	-0.2249	-0.2338
B	*a*	-17.46	-21.51	-23.23	-23.75	0.1196	0.1618	0.1873	0.1970	-0.1643	-0.2124	-0.2312	-0.2363
	d	-18.49	-22.00	-23.34	-23.76	0.1687	0.1693	0.1940	0.2018	-0.2011	-0.2382	-0.2485	-0.2482
	i	-15.36	-18.97	-21.60	-23.07	0.1486	0.1547	0.1838	0.1964	-0.1446	-0.1838	-0.2147	-0.2337
C	*h*	-23.24	-23.79	-23.90	-23.94	0.2051	0.2015	0.2042	0.2040	-0.2629	-0.2466	-0.2399	-0.2377
	l	-22.97	-23.76	-23.90	-23.94	0.2114	0.2023	0.2041	0.2037	-0.2557	-0.2430	-0.2392	-0.2375
D	*e*	-22.14	-23.57	-23.85	-23.93	0.1911	0.1903	0.1988	0.2014	-0.2110	-0.2301	-0.2369	-0.2376
	j	-21.21	-23.42	-23.85	-23.93	0.1305	0.1971	0.2020	0.2032	-0.1931	-0.2304	-0.2379	-0.2375

3.5. Bending of an Unlimited Wedge by a Concentrated Moment Applied to Its Vertex (Inglis Problem).

Let us consider an unlimited wedge with thickness h=1m and moment M applied to its vertex shown in Figure 7a: r, β – polar coordinates of the point. This problem has an analytical solution [22]:

$$\sigma_r = \frac{2M\sin(2\beta)}{r^2\left(2\alpha\cos(2\alpha)-\sin(2\alpha)\right)},$$
$$\tau_{r\beta} = \frac{2M(\cos(2\alpha)-\cos(2\beta))}{r^2\left(2\alpha\cos(2\alpha)-\sin(2\alpha)\right)} \qquad (70)$$

Let us consider the area $R \le 24$m, α=22.5° and specify the boundary conditions shown in Figure 7b. According to the Saint-Venant's principle these constraints will not have a significant effect on the results, since we will consider points A(4,-22°) and B(4,0°). Analytical solutions according to (70):

$\sigma_{\rho,A}$ = 0.582474 kPa, $\tau_{r\beta,B}$ = 0.120634 kPa.

We take:

$E = 3.0\cdot10^7$ kPa, ν = 0.2, h=1m, M=–1kN.

Radii of points in the design models in Figure 8: 0.5, 0.625, 1, 1.75, 2.5, 3.25, 4, 4.75, 5.5, 6.5, 7.75, 9.25, 11,13, 15.5, 18, 21, 24.

Table 5 shows the results of calculations only for elements with degrees of freedom ω_z, since they are incorrect for elements with quasi-rotational degrees of freedom.

Let us consider the area $R \le 24$m, α=22.5° and specify the boundary conditions shown in Figure 7b. According to the Saint-Venant's principle these constraints will not have a significant effect on the results, since we will consider points A(4,-22°) and B(4,0°). Analytical solutions according to (70):

$\sigma_{\rho,A}$ = 0.582474 kPa, $\tau_{r\beta,B}$ = 0.120634 kPa.

We take:

$E = 3.0\cdot10^7$ kPa, ν = 0.2, h=1m, M=–1kN.

Radii of points in the design models in Figure 8: 0.5, 0.625, 1, 1.75, 2.5, 3.25, 4, 4.75, 5.5, 6.5, 7.75, 9.25, 11,13, 15.5, 18, 21, 24.

Table 5 shows the results of calculations only for elements with degrees of freedom ω_z, since they are incorrect for elements with quasi-rotational degrees of freedom.

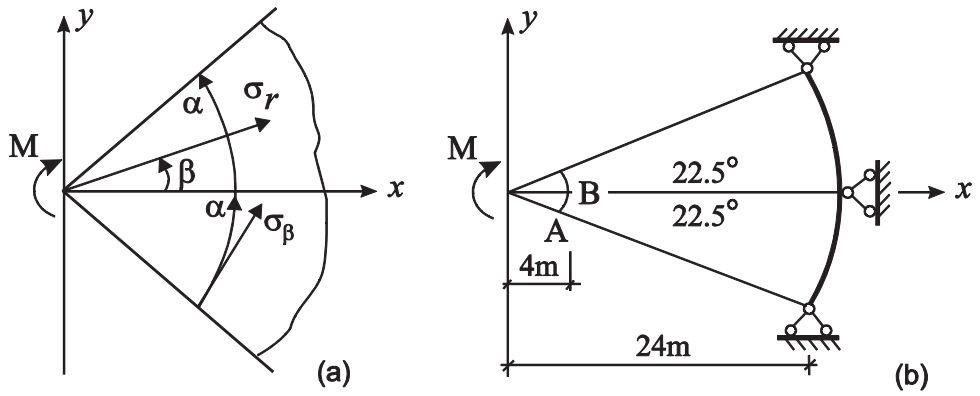

Figure 7. Inglis problem.

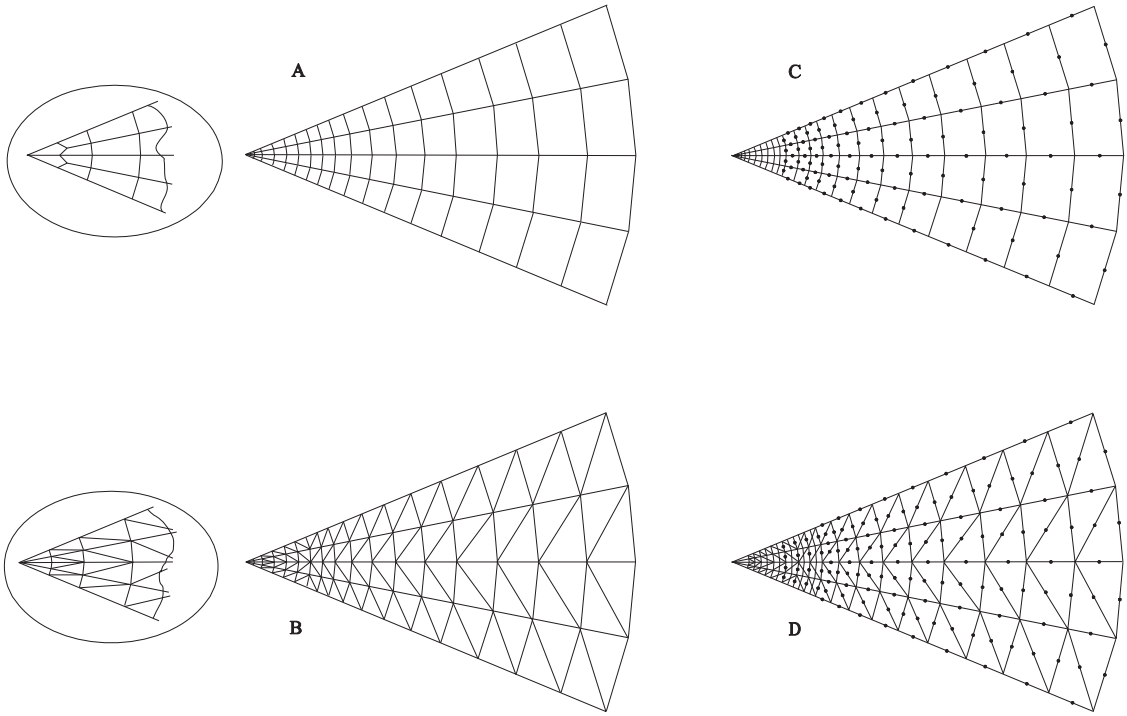

Figure 8. Wedge design models.

Table 5. Stresses in the Inglis problem.

Mesh type	Element	Stresses $\sigma_{r,A}$ (Pa)				Stresses $\tau_{r\beta,B}$ (Pa)			
		Mesh				Mesh			
		A	A2	A4	A8	A	A2	A4	A8
A	*g*	0.6108	0.5909	0.5851	0.5834	0.0914	0.1172	0.1216	0.1218
	k	0.5759	0.5781	0.5801	0.5812	0.1216	0.1208	0.1208	0.1207
C	*d*	0.6578	0.6108	0.5940	0.5875	0.1135	0.1121	0.1164	0.1185
	i	0.5541	0.5761	0.5811	0.5822	0.1043	0.1217	0.1232	0.1224
B	*h*	0.5637	0.5784	0.5816	0.5823	0.1522	0.1263	0.1220	0.1210
	l	0.5737	0.5809	0.5821	0.5824	0.1414	0.1259	0.1219	0.1210
D	*e*	0.6066	0.5892	0.5843	0.5830	0.1283	0.1244	0.1230	0.1220
	j	0.5418	0.5706	0.5791	0.5816	0.1220	0.1213	0.1209	0.1207

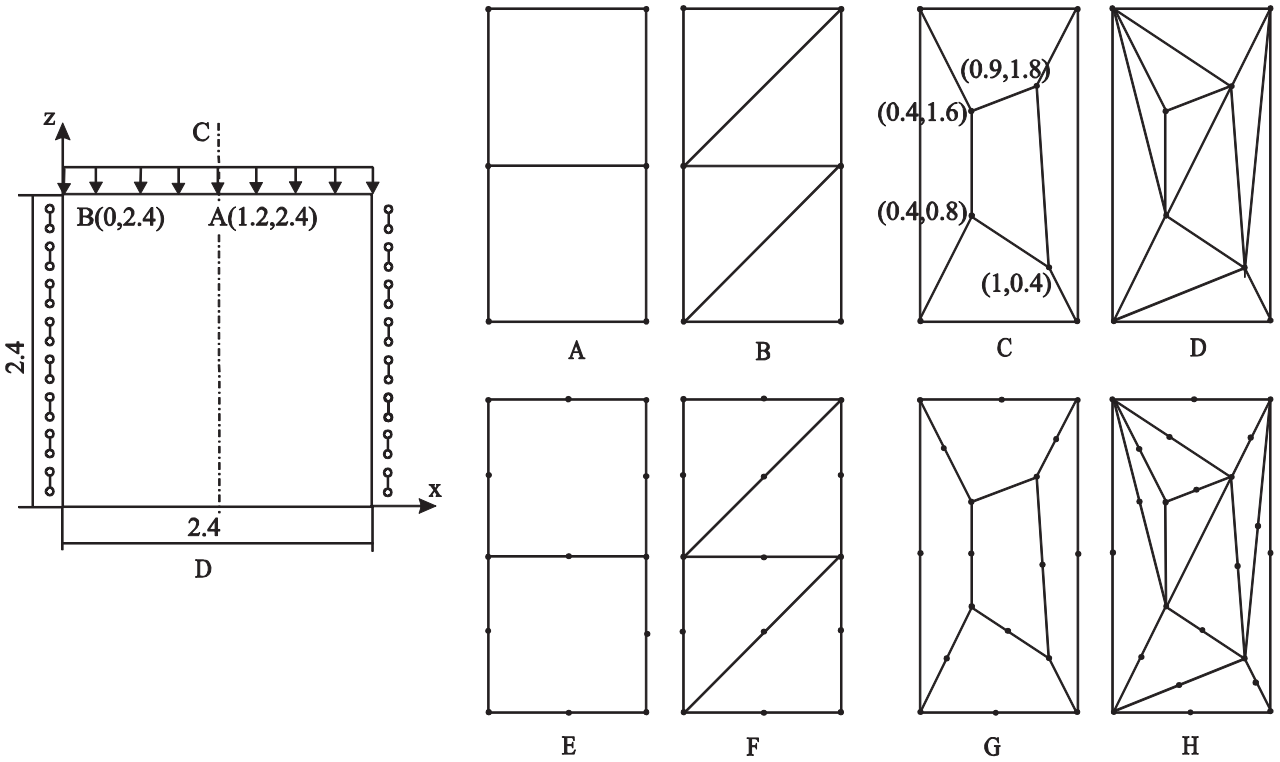

Figure 9. Deep beam and its design models.

3.6. Bending of a Rectangular Deep Beam.
Let us consider a square deep beam rigidly suspended on the sides x=0 and x=2.4 (Figure 9) and subjected to a uniformly distributed load p applied to its upper edge. This problem has an analytical solution in series, given in [23]. Displacement values are calculated with high accuracy in [24] for a square plate with the following characteristics: E=2.65·MPa, ν=0.15, h=0.1m, p=500N/m: w_A=–3.763392mm, u_B=2.210055mm.
The calculation is performed only for the half of the deep beam taking into account the axis of symmetry CD and the following boundary conditions: $w|_{x=0}= u|_{x=1.2}=\omega/\theta|_{x=1.2}=0$. Design models are shown in Fig. 9. Models C and D are the same as those used for patch tests [20]. Calculation results are given in Table 6.

4. CONCLUSIONS

The conducted numerical experiments have confirmed theoretical foundations for creating finite elements:

- elements with quasi-rotational degrees of freedom ***a,b,c*** and incompatible elements ***d,f,g*** yield almost identical results in displacements and stresses;
- elements ***a,b,c*** can yield incorrect results in rotation angles;
- *compatible* elements ***i,k*** yield *slightly worse* results compared to elements ***a,b,c,d,f,g***;
- as expected, elements with intermediate nodes on the sides ***e,h,j,l*** have yielded the best numerical results. And compatible elements ***j,l*** are unparalleled;
- all elements with degrees of freedom ω_z enable to calculate structures subjected to both concentrated and uniformly distributed moments.

It is now interesting to study the application of the given approximations when creating shell elements (especially in combined design models with bar elements).

Table 6. Displacements in the rigidly suspended deep beam.

Mesh type	Element	Displacements w_A (mm)				Displacements u_B (mm)			
		Mesh				Mesh			
		2x2	4x4	8x8	16x16	2x2	4x4	8x8	16x16
A	*b*	-3.4643	-3.6726	-3.7415	-3.7580	1.9846	2.1234	2.1739	2.1966
	c	-3.4603	-3.6686	-3.7414	-3.7580	1.8881	2.0835	2.1546	2.1870
	f	-3.5971	-3.6802	-3.7410	-3.7577	2.0216	2.0975	2.1564	2.1875
	g	-3.5344	-3.6762	-3.7395	-3.7573	1.8855	2.0341	2.1258	2.1725
	k	-3.3881	-3.6433	-3.7312	-3.7554	1/9479	2.0749	2.1505	2.1858
B	*a*	-3.2005	-3.6080	-3.7249	-3.7547	1.8805	2.0160	2.1214	2.1715
	d	-3.3494	-3.6562	-3.7377	-3.7582	2.1242	2.1274	2.1736	2.1967
	i	-3.0276	-3.5946	-3.7042	-3.7468	1.9472	2.0158	2.1133	2.1674
C	*b*	-3.1204	-3.6785	-3.7518	-3.7627	1.4033	1.9437	2.0779	2.1411
	c	-3.1483	-3.6716	-3.7507	-3.7626	1.5706	1.9523	2.0554	2.1257
	g	-3.1957	-3.6065	-3.7582	-3.7745	1.6774	1.6550	1.8636	2.0106
	k	-2.8401	-3.4950	-3.6285	-3.7053	1.8166	2.0413	2.1162	2.1461
D	*a*	-3.0684	-3.5233	-3.6936	-3.7464	1.7172	1.9280	2.0795	2.1497
	d	-3.2120	-3.5619	-3.7015	-3.7492	2.0067	2.0686	2.1351	2.1736
	i	-2.7636	-3.1829	-3.3407	-3.4860	1.8346	1.8803	1.9712	2.0734
E	*h*	-3.8112	-3.7866	-3.7752	-3.7677	1.9724	2.1122	2.1663	2.1923
	l	-3.7435	-3.7543	-3.7630	-3.7635	1.8486	2.0507	2.1359	2.1770
G	*h*	-3.8661	-3.8615	-3.8079	-3.7799	1.6800	1.9761	2.0908	2.1497
	l	-3.5164	-3.7586	-3.7651	-3.7639	1.3827	1.8735	2.0504	2.1316
F	*e*	-3.8582	-3.7694	-3.7593	-3.7621	1.7710	2.0022	2.1109	2.1648
	j	-3.4784	-3.7437	-3.7620	-3.7634	1.6815	1.9797	2.1015	2.1600
H	*e*	-3.6114	-3.7890	-3.8003	-3.7818	1.7490	1.9895	2.1021	2.1594
	j	-3.4959	-3.7713	-3.7742	-3.7665	1.4127	1.8596	2.0539	2.1392

REFERENCES

1. **Novozhilov V.V.** Osnovy nelineynoy teorii uprugosti [Foundations of the Nonlinear Theory of Elasticity]. Moskow, Gostekhteorizdat, 1948, 333 pages (in Russian).
2. **Allman D.J.** A compatible triangular element including vertex rotations forplane elasticity analysis. // *Computers and Structures*, 1984, Vol. 19(1-2), pp. l-8.
3. **Allman D.J.** A quadrilateral finite element including vertex rotations for plane elasticity analysis. // *International Journal for Numerical Methods in Engineering*, 1988, Vol. 26(3), pp. 717-730.
4. **Cook R.D.** On the Allman triangle and a related quadrilateral element. // *Computers and structures*, 1986, Volume 22(6), pp. 1065-1067.
5. **MacNeal R.H., Harder R.L.** A refined four-noded membrane element with rotational degrees of freedom. // *Computers and Structures*, 1988, Vol. 28(1), pp. 75-84.
6. **Karpilovskyi V.S.** Novyy sovmestnyy chetyrekhugolnyy konechnyy element balki-stenki s vrashchatelnymi stepenyami svobody [New compatible quadrangular deep beam finite element with rotational degrees of freedom]. // *Materials of the II International Scientific and Practical Conference "Suchasni` metodi i problemno-oriyintovani kompleksi rozrakhunku konstrukczij i yikh zastosuvannya u proyektuvanni i navchalnomu proczesi" ["Modern Methods*

and Problem-Oriented Complexes for Structural Analysis and Their Application in Design and Educational Process"]. Kyiv, September 2018, pp. 57-59 (in Russian)

7. **Wilson E.L., Ibrahimbegovic A.** Thick shell and solid elements with independent rotation fields. // *International Journal for Numerical Methods in Engineering*, 1991, Volume 31(7), pp. 1393-1414.
8. **Zhang H., Kuong J.S.** Eight-node membrane element with drilling degrees of freedom for analysis of in-plane stiffness of thick floor plates. // *International Journal for Numerical Methods in Engineering*, 2008, Volume 76(13). pp. 2117-2136.
9. **Yunus S., Saigal S., Cook R.** On improved hybrid finite elements with rotational degrees of freedom. //Interntional journal for numerical methods in ingineering, 1989, Vol. 28(4), pp. 785-800. DOI: 10.1002/nme.1620280405
10. **Choo Y.S., Choi N., Lee B.C.** Quadrilateral and triangular plate elements with rotational degrees of freedom based on the hybrid Trefftz method. // *Finite Elements in Analysis and Design*, 2006, Volume 42(11), pp. 1002-1008.
11. **Cook R.** A plane hybrid element with rotational d.o.f. and adjustable stiffness. // *International Journal for Numerical Methods in Engineering*, 1987, Volume 24(8), pp. 1499-1508.
12. **Fellipa C.A.** A study of optimal membrane triangles with drilling freedoms. // *Computer Methods in Applied Mechanics and Engineering*, 2003, Volume 192(16-18), pp. 2125-2168.
13. **Chen X.M., Cen S., Sun J.Y., Li Y.G.** Four-Node Generalized Conforming Membrane Elements with Drilling DOFs Using Quadrilateral Area Coordinate Methods. // *Mathematical Problems in Engineering*, 2015, Volumes 3-4, pp. 1-13.
14. **Britvin E.I., Peysin A., Eisenberger M.** Deformiruyemyy v svoyey ploskosti chetyrekhugolnyy konechnyy element s vrashchatelnymi stepenyami svobody v uzlakh. Chast 2. Proizvolnyy chetyrekhugolnik [Quadrangular finite element deformable in its plane with rotational degrees of freedom in the nodes. Part 2. Arbitrary quadrangle]. // *Structural Mechanics and Analysis of Constructions*, 2018, Volume 4, pp. 50-54 (in Russian).
15. **Karpilovskyi V.S.** Issledovanie i konstruirovanie nekotorykh tipov konechnykh elementov dlya zadach stroitel`noj mekhaniki. [Study and design of some types of finite elements for the structural mechanics problems]. // PhD Thesis, National transport university (KADI), Kyiv, 1982, 179 pages (in Russian)
16. **Evzerov I.D.** Oczenki pogreshnosti po peremeshheniyam pri ispol`zovanii nesovmestny`kh konechny`kh e`lementov [Estimates of the error in displacements when using incompatible finite elements]. // *Chislennye metody mekhaniki sploshnoj sredy [Numerical methods of continuum mechanics]*, Novosibirsk, 1983, Volume 14(5), pp. 24-31 (in Russian).
17. **Gorodetsky A.S., Karpilovskyi V.S.** Metodicheskiye pekomendatsii po issledovaniyu i konstpuipovaniyu konechnyx elementov [Methodological recommendations for the study and construction of finite elements]. Kyiv, NIIASS, 1981, 48 pages (in Russian).
18. **Irons B.M., Razzaque A.** Experience with the path test. // In: The Matematical Foundations of the Finite Element Method with Application to Partial Differential Equations, Academic Press, 1972, pp. 557-587.
19. **Strang G., Fix G.** An Analysis of the Finite Element Method. Prentice Hall, Englewood Cliffs, N.J., 1973.
20. **Aubin J.P.** Approximation of Elliptic Boundary-Value Problems. John Wiley & Sons, N.Y., 1972.
21. **Macneal R.H., Harder R.L.** A proposed standard set of problems to test finite

element accuracy. // *Finite Elements in Analysis and Design*, 1985, Volume 1, pp. 3-20.
22. **Rekach V.G.** Rukovodstvo k resheniyu zadach po teorii uprugosti [Guide to Solving Problems of Elasticity]. Moscow, Vysha shkola, 1977, 216 pages (in Russian).
23. **Kalmanok A.S.** Raschet balok-stenok [Analysis of Deep Beams]. Moscow, Gosstroyizdat, 1956, 151 pages (in Russian).
24. **Gorodetsky A.S., Karpilovskyi V.S.** O svyazi metoda konechnykh elementov s variatsionno-raznostnymi metodami [On the relation between the finite element method and the variation difference methods]. // *Strength of Materials and Theory of Structures*, 1974, Volume 24, pp. 32-42. (in Russian).

СПИСОК ЛИТЕРАТУРЫ

1. **Новожилов В.В.** Основы нелинейной теории упругости. – М.: Гостехтеориздат, 1948. – 333 с.
2. **Allman D.J.** A compatible triangular element including vertex rotations forplane elasticity analysis. // *Computers and Structures*, 1984, Vol. 19(1-2), pp. l-8.
3. **Allman D.J.** A quadrilateral finite element including vertex rotations for plane elasticity analysis. // *International Journal for Numerical Methods in Engineering*, 1988, Vol. 26(3), pp. 717-730.
4. **Cook R.D.** On the Allman triangle and a related quadrilateral element. // *Computers and structures*, 1986, Volume 22(6), pp. 1065-1067.
5. **MacNeal R.H., Harder R.L.** A refined four-noded membrane element with rotational degrees of freedom. // *Computers and Structures*, 1988, Vol. 28(1), pp. 75-84.
6. **Карпиловский В.С.** Новый совместный четырехугольный конечный элемент балки-стенки с вращательными степенями свободы. // *Сборник трудов II Международной научно-практической конференции «Сучасні методи і проблемно-орієнтовані комплекси розрахунку конструкцій і їх застосування у проектуванні і навчальному процесі» [Современные методы и проблемно-ориентированные комплексы расчета конструкций и их применение в проектировании и учебном процессе]*. (г. Киев, 26-27 сентября 2018 года), Киев, 2018, с. 57-59.
7. **Wilson E.L., Ibrahimbegovic A.** Thick shell and solid elements with independent rotation fields. // *International Journal for Numerical Methods in Engineering*, 1991, Volume 31(7), pp. 1393-1414.
8. **Zhang H., Kuong J.S.** Eight-node membrane element with drilling degrees of freedom for analysis of in-plane stiffness of thick floor plates. // *International Journal for Numerical Methods in Engineering*, 2008, Volume 76(13). pp. 2117-2136.
9. **Yunus S., Saigal S., Cook R.** On improved hybrid finite elements with rotational degrees of freedom. //Interntional journal for numerical methods in ingineering, 1989, Vol. 28(4), pp. 785-800. DOI: 10.1002/nme.1620280405
10. **Choo Y.S., Choi N., Lee B.C.** Quadrilateral and triangular plate elements with rotational degrees of freedom based on the hybrid Trefftz method. // *Finite Elements in Analysis and Design*, 2006, Volume 42(11), pp. 1002-1008.
11. **Cook R.** A plane hybrid element with rotational d.o.f. and adjustable stiffness. // *International Journal for Numerical Methods in Engineering*, 1987, Volume 24(8), pp. 1499-1508.
12. **Fellipa C.A.** A study of optimal membrane triangles with drilling freedoms. // *Computer Methods in Applied Mechanics and Engineering*, 2003, Volume 192(16-18), pp. 2125-2168.
13. **Chen X.M., Cen S., Sun J.Y., Li Y.G.** Four-Node Generalized Conforming

Membrane Elements with Drilling DOFs Using Quadrilateral Area Coordinate Methods. // *Mathematical Problems in Engineering*, 2015, Volumes 3-4, pp. 1-13.
14. **Бритвин Е.И., Пейсин А., Эйсенбергер М.** Деформируемый в своей плоскости четырехугольный конечный элемент с вращательными степенями свободы в узлах. Часть 2. Произвольный четырехугольник. // *Строительная механика и расчет сооружений*, 2018, №4, с. 50-54.
15. **Карпиловский В.С.** Исследование и конструирование некоторых типов конечных элементов для задач строительной механики. Диссертация на соискание ученой степени кандидата технических наук по специальности 01.02.03 – «Строительная механика». – Киев: Национальный транспортный университет (КАДИ), 1982. – 179 с.
16. **Евзеров И.Д.** Оценки погрешности по перемещениям при использовании несовместных конечных элементов // *Численные методы механики сплошной среды*, 1983, том 14, №5, с. 24-31.
17. **Городецкий А.С., Карпиловский В.С.** Методические рекомендации по исследованию и конструированию конечных элементов. Киев: НИИАСС, 1981. – 48 с.
18. **Irons B.M., Razzaque A.** Experience with the path test. // In: The Mathematical Foundations of the Finite Element Method with Application to Partial Differential Equations, Academic Press, 1972, pp. 557-587.
19. **Стренг Г., Фикс Дж.** Теория метода конечных элементов – М.: Мир, 1977. – 349 с.
20. **Обен Ж.-П.** Приближенное решение эллиптических краевых задач. – М.: Мир, 1977. – 384с.
21. **Macneal R.H., Harder, R.L.** A proposed standard set of problems to test finite element accuracy. // *Finite Elements in Analysis and Design*, 1985, Volume 1, pp. 3-20.
22. **Рекач В.Г.** Руководство к решению задач по теории упругости. – М.: Высшая школа, 1977. – 216 с.
23. **Калманок А.С.** Расчет балок-стенок. – М.: Госстройиздат, 1956. – 151с.
24. **Городецкий А.С., Карпиловский В.С.** О связи метода конечных элементов с вариационно-разностными методами. // *Сопротивление материалов и теория сооружений*, Выпуск 24, 1974, с. 32-42.

Viktor S. Karpilovskyi, PhD, Associated Professor, Director of IT Company ScadGroup Ltd.; 03037, 3A Osvity street, office 2, Kiev 03037, Ukraine;
phone: +38(044)2497191(3);
E-mail: kvs@scadsoft.com; http://www.scadsoft.com;
ORCID: 0000-0002-9437-0373.

Карпиловский Виктор Семенович, кандидат технических наук, старший научный сотрудник, директор ООО ScadGroup; 03037, Украина, г.Киев, ул. Освіти(Просвещения), д.3а, оф. 2;
тел: +38(044)2497191(3);
E-mail: kvs@scadsoft.com; http://www.scadsoft.com;
ORCID : 0000-0002-9437-0373.